© 2022. Published by The Company of Biologists Ltd | Development (2022) 149, dev200891. doi:10.1242/dev.200891

RESEARCH ARTICLE

Nutrition-dependent juvenile hormone sensitivity promotes flight-muscle degeneration during the aphid dispersal-reproduction transition

Yu Bai[1,2], Xiao-Jin Pei[1], Ning Ban[3], Nan Chen[1], Su-Ning Liu[1], Sheng Li[1,*] and Tong-Xian Liu[4,*]

ABSTRACT

In insects, the loss of flight typically involves a dispersal-reproduction transition, but the underlying molecular mechanisms remain poorly understood. In the parthenogenetic pea aphid *Acyrthosiphon pisum*, winged females undergo flight-muscle degeneration after flight and feeding on new host plants. Similarly, topical application of a juvenile hormone (JH) mimic to starved aphids also induces flight-muscle degeneration. We found that feeding preferentially upregulated the expression of the JH receptor gene *Met* and a JH-inducible gene, *Kr-h1*, in the flight muscles, and, thus, enhanced tissue-specific JH sensitivity and signaling. RNAi-mediated knockdown of *Kr-h1* prevented flight-muscle degeneration. Likewise, blocking nutritional signals by pharmacological inhibition of the target of rapamycin complex 1 (TORC1) impaired JH sensitivity of the flight muscles in feeding aphids and subsequently delayed muscle degeneration. RNA-sequencing analysis revealed that enhanced JH signaling inhibited the transcription of genes involved in the tricarboxylic acid cycle, likely resulting in reduction of the energy supply, mitochondrial dysfunction and muscle-fiber breakdown. This study shows that nutrient-dependent hormone sensitivity regulates developmental plasticity in a tissue-specific manner, emphasizing a relatively underappreciated mechanism of hormone sensitivity in modulating hormone signaling.

KEY WORDS: Flight muscle, Developmental plasticity, Juvenile hormone sensitivity, TCA cycle, Mitochondria, *Acyrthosiphon pisum*

INTRODUCTION

Dispersal is an evolutionary driver that fundamentally shapes the distribution, abundance and diversity of insects, and plays a key role in their persistence in heterogeneous habitats (Weigang and Kisdi, 2015). However, dispersal is associated with high energetic costs (Bonte et al., 2012), which require trade-offs with other physiological activities such as reproduction (Guo et al., 2016). After locating a suitable colonization environment, insects that have dispersed are able to integrate external and internal environmental signals and maintain a systemic energy balance, while shifting resources toward the production of offspring instead of flight (Zera and Denno, 1997; Zhang et al., 2019).

A life-history trade-off exists between flight capability and reproduction in many wing-dimorphic insects (Guerra, 2011). Aphids can develop either with or without wings. Unwinged aphids remain on the host plant and feed and reproduce there. Winged aphids are induced by environmental cues, such as crowding and reduced nutritional quality. When a winged aphid molts into the adult form, the aphid does not feed before flight. After the aphid flies to a new host plant and begins feeding, the flight muscles (which represent a valuable nutritional resource) degenerate, and presumably the freed resources are redirected to the development of embryos (Brisson, 2010; Johnson, 1959; Kobayashi and Ishikawa, 1993). Thus, muscle degeneration is an adaptive strategy to maximize reproductive success. It was previously shown that topical application of juvenile hormone (JH) induced flight-muscle degeneration, which resembled feeding-dependent degeneration (Kobayashi and Ishikawa, 1994). Nevertheless, the regulatory mechanisms underlying flight-muscle degeneration in aphids when flight is unnecessary remains poorly understood.

Hormonal signals commonly integrate environmental cues (such as nutrition) to mediate a range of developmental processes (Nijhout, 1999; Beldade et al., 2011; Simpson et al., 2011; Johnson et al., 2014; Zhang et al., 2019). Besides regulating metamorphosis and reproduction (Jindra et al., 2013; Roy et al., 2018), JH plays key roles in regulating developmental plasticity in insects, including dispersal-reproduction trade-offs (Gotoh et al., 2014; Reiff et al., 2015; Miura, 2018). Target of rapamycin complex 1 (TORC1) is a well-conserved nutrient sensor (mainly amino acids) in the insect fat body, with a prominent role in linking systemic nutritional conditions to local cellular physiology in peripheral tissues (Colombani et al., 2003; Géminard et al., 2009; Howell and Manning, 2011; Li et al., 2019b). Eukaryotic initiation factor 4E-binding protein (4EBP) is a key TORC1 target, and the TORC1-mediated phosphorylation of 4EBP is regarded as an indicator of TORC1 activity (Hietakangas and Cohen, 2009). Recent studies have also implicated the TORC1 pathway in the stimulation of JH biosynthesis via upregulation of the expression of juvenile hormone acid methyltransferase (*JHAMT*) (Maestro et al., 2009; Pérez-Hedo et al., 2013; Lu et al., 2016; Zhu et al., 2020), which encodes a rate-limiting enzyme for JH biosynthesis and is expressed specifically in the corpora allata located in insect heads (Shinoda and Itoyama, 2003; Wen et al., 2015). In addition to systemic biosynthesis, gene expression levels of other molecules required for JH signaling, such as the JH receptor *Met* (Konopova and Jindra, 2007), also affect JH regulatory efficacy. JH/Met induces the expression of the JH primary-response gene *Kr-h1*, which

[1]Guangdong Provincial Key Laboratory of Insect Development Biology and Applied Technology, Institute of Insect Science and Technology, School of Life Sciences, South China Normal University, Guangzhou 510631, China. [2]State Key Laboratory of Crop Stress Biology for Arid Areas and Key Laboratory of Integrated Pest Management on the Loess Plateau of Ministry of Agriculture, Northwest A&F University, Yangling 712100, China. [3]Key Lab of Integrated Crop Pest Management of Shandong Province, College of Plant Health and Medicine, Qingdao Agricultural University, Qingdao 266109, China. [4]Institute of Entomology, Guizhou University, Guiyang 550025, China.

*Authors for correspondence (tx.liu@gzu.edu.cn; lisheng@scnu.edu.cn)

S.L., 0000-0002-4217-2367; T.-X.L., 0000-0002-7686-0686

Handling Editor: Cassandra Extavour
Received 3 May 2022; Accepted 28 June 2022

Development (2022) 149, dev200891. doi:10.1242/dev.200891

conservatively reflects the degree of JH signaling (Jindra et al., 2013; Li et al., 2019a).

To examine how nutrition and JH interact to regulate flight-muscle degeneration, we focused on the winged female morph of pea aphids. We report that TORC1 mediates nutritional signaling and enhances the expression of *Met* and *Kr-h1*, and thus JH sensitivity, specifically in the flight muscles, leading to the restriction of energy supplies and the induction of flight-muscle degeneration in winged aphids. Our results highlight hormone sensitivity as an important tissue-specific regulatory mechanism of developmental transitions in the insect life history.

RESULTS

Feeding and JH application induce mitochondrial disruption and flight-muscle-fiber breakdown

Our cage studies indicated that newly molted, winged female aphids remained static for 24 h (resting mode). The females then flew toward the light and maintained an active state within a 16 h photoperiod (flight mode). Females that successfully located plants for colonization then initiated feeding (settling mode), which resulted in fully distended abdomens by 48-60 h (colonization mode). By 72-84 h post eclosion, nearly all females began to produce nymphs (larviposition mode) (Fig. 1A-A″).

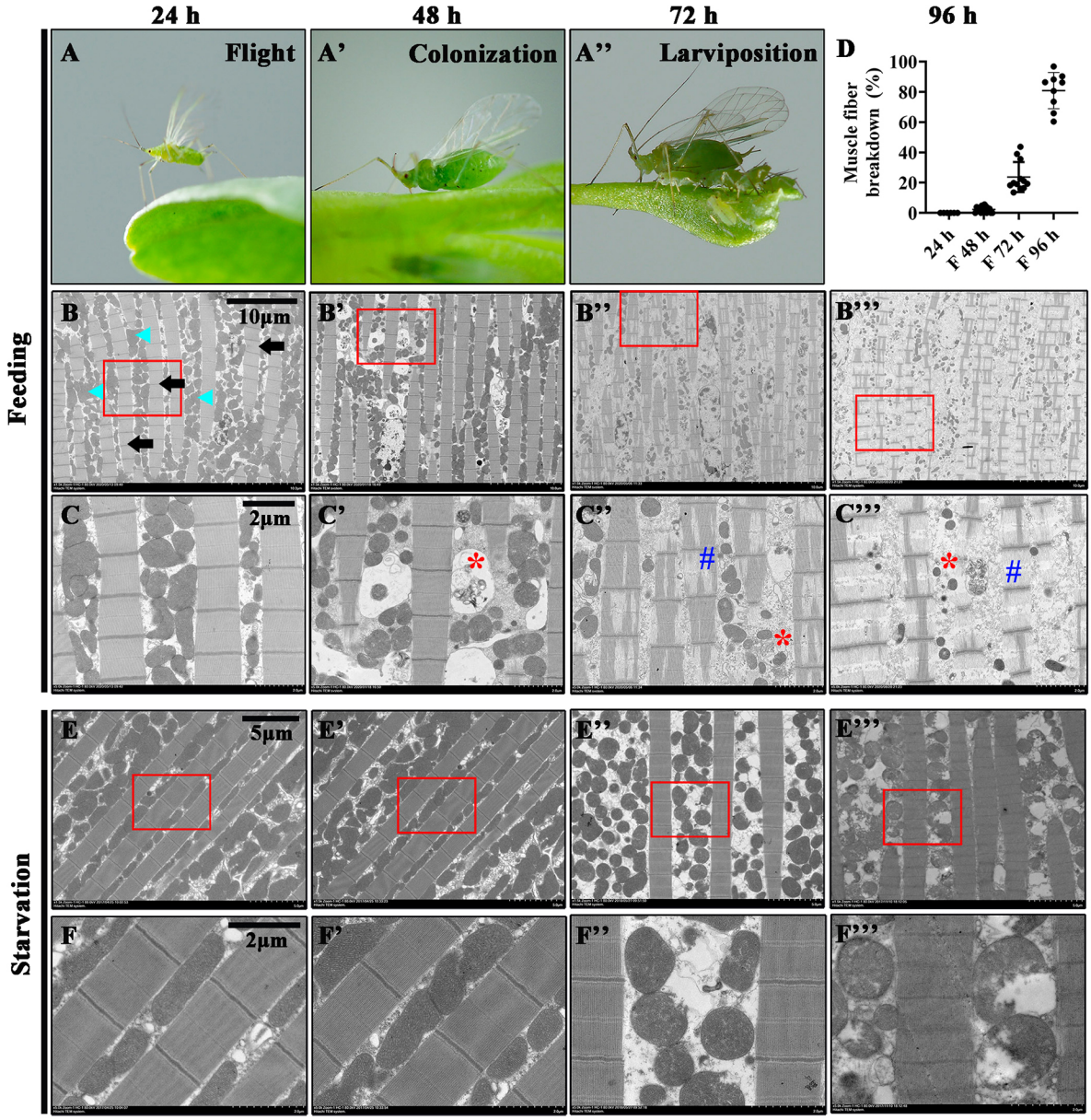

Fig. 1. Histological observation of the flight muscles in winged *A. pisum* morphs under feeding and starved conditions post eclosion. (A-A″) Under experimental feeding conditions, the aphids present a typical flight (A), colonization (A′) and larviposition (A″) mode at 24, 48 and 72 h post eclosion, respectively. (B-F) Transmission electron microscopy (TEM) observations of the flight muscles from 24 h to 96 h under feeding (B-B‴) or starvation (E-E‴) conditions. Detailed magnifications of the sections in the red boxes highlighting muscle fibers and mitochondria in panels B-B‴ and E-E‴ are shown in C-C‴ and F-F‴, respectively. Blue arrowheads indicate mitochondria, black arrows indicate muscle fibers, red asterisks indicate disrupted mitochondria and blue hashes indicate broken muscle fibers. Quantitative statistics (D) of muscle fiber breakdown in the feeding (F) condition, shown as the percentage of 'blank muscle fiber area' to the total muscle fiber area; three images of each available TEM sample were selected for the area statistics, data are indicated as mean±s.e.m. Three, six, six and three aphids were examined at 24, 48, 72 and 96 h, respectively, under feeding or starvation conditions. Individual representative phenotypic images for two, five, four and three samples from the examined aphids of each mode, respectively, are exhibited here. Other TEM samples with representative phenotypes for each mode are shown in Figs S1 and S2. More than two-thirds of the aphids in each mode display representative characteristics.

Development (2022) 149, dev200891. doi:10.1242/dev.200891

Examining the flight muscles by transmission electron microscopy (TEM) showed that 24-h-old females in flight mode possessed large, irregularly shaped mitochondria that were highly abundant between muscle fibers (Fig. 1B-D; Fig. S1A). The flight muscles of females in colonization mode (48 h) contained irregularly shaped mitochondria with condensed matrices, but exhibited no obvious defects in the muscle fibers (Fig. 1B′,C′,D; Fig. S1B). Subsequently, muscle fibers were severely degenerated with few mitochondria present in larviposition-mode females (72 h) (Fig. 1B″,C″,D; Fig. S1C). Until 96 h after eclosion, almost all the flight muscles were degenerated in feeding aphids (Fig. 1B‴,C‴,D; Fig. S1D). In contrast, when winged females were starved after eclosion, the flight-muscle fibers remained morphologically intact over a 96 h observation period, although mitochondria shifted from a flattened to a circular morphology (Fig. 1E-F‴; Fig. S2A-D). We further noted that in winged female aphids, muscle degeneration induced by feeding was present in the flight muscles but not the leg muscles, in which JH signaling (as indicated by gene expression levels of *Met* and *Kr-h1*) slightly decreased in feeding aphids compared with that in starved aphids (Fig. S3A,B).

We then examined whether exogenous JH plays a role similar to feeding in inducing morphological changes in the flight muscles during starvation. Topical application of methoprene (a JH mimic) significantly induced *Kr-h1* expression in the flight muscles at 6-48 h after treatment during starvation (Fig. 2A). Methoprene application also induced flight-muscle degeneration; similarly, mitochondrial disruption occurred earlier than muscle-fiber breakdown (Fig. 2B-F; Fig. S4A-D). Although methoprene induced *Kr-h1* expression in the leg muscles, the induction efficiencies were significantly lower than those in the flight muscles at 12 h after application (Fig. S5A). Notably, methoprene application did not significantly induce leg-muscle degeneration (Fig. S5B). It is likely that feeding activates tissue-specific JH signaling and induces flight-muscle degeneration in winged female pea aphids.

Feeding-dependent JH sensitivity induces tissue-specific flight-muscle degeneration

We compared the transcriptional dynamics of genes with roles in JH biosynthesis and signaling between winged morph aphids that were fed or starved. We firstly employed RNA-sequencing (RNA-seq) analysis of the heads to compare the transcriptional changes of all genes involved in JH biosynthesis between winged aphids in ‘flight’ (24 h post eclosion) and ‘colonization’ (60 h post eclosion) modes. The results showed that there were no significant changes in expression in any of the JH-biosynthesis genes in the heads between the two modes (Fig. S6A). The pea aphid might have four *JHAMT* homologs; however, there is no clear evidence showing which gene(s) might be the functional *JHAMT* homolog(s). *JHAMT1*, *JHAMT2* and *JHAMT3* were annotated in the transcriptome, and we further verified their expression levels using quantitative real-time PCR (qPCR) under the starvation versus feeding regime. The relative transcript abundance of *JHAMT1-3* in the heads of fed and starved winged females was similar up to 72 h post eclosion (flight-muscle degeneration had already initiated by this time), but diverged post 72 h. The transcript abundance of *JHAMT2* increased in feeding aphids, whereas that of *JHAMT3* decreased in starved aphids, and significant differences in JHAMT expression were observed until 96 h post eclosion between feeding and starved females (Fig. 2G-I). Conversely, the relative transcript abundance of *Met* and *Kr-h1* was significantly higher in the thoraxes (which are almost filled with flight muscles) of fed versus starved females by 48-96 h post eclosion (Fig. 2J,K).

The temporal expression patterns of key genes of the JH pathway implied that the upregulated expression of the JH intracellular receptor gene *Met* resulted in the increase of JH signaling, even though JH-biosynthesis genes were not significantly upregulated during the colonization of winged aphids. Given these outcomes, we further explored the spatial expression of *Met* and *Kr-h1*. We compared *Met* and *Kr-h1* expression in the heads, thoraxes, ovaries, fat body and legs with that in the flight muscles of winged females at 60 h post eclosion under starved or fed conditions. The results showed that each gene was preferentially expressed in the thoraxes and flight muscles of the fed winged aphids, especially *Met* (Fig. 2L,M).

Temporal and spatial expression patterns of JH biosynthesis and signaling genes demonstrated that the transcription of *Met* was specifically activated in the flight muscles of winged aphids during the process of colonization. It is reasonable to assume that many intracellular receptors contribute to the sensitive detection of JH levels and subsequently induce JH nuclear signals. To verify this hypothesis, we topically applied the JH mimic on the winged aphids during colonization mode and detected the expression levels of *Kr-h1* in various tissues using qPCR 12 h after the treatment. The results showed that JH induced the expression of *Kr-h1* more efficiently in the flight muscles than in any other tissues of feeding winged aphids (Fig. 2N).

Subsequently, we employed RNA interference (RNAi) to decrease the feeding-induced gene expression of *Met* and *Kr-h1*. *Met* RNAi was not successfully achieved in the pea aphid, whereas *Kr-h1* RNAi resulted in ∼50% reduction in gene expression in the flight muscles of feeding winged aphids 48 h after the treatment (Fig. 3A). Importantly, aphids treated with *Kr-h1* RNAi exhibited delayed mitochondrial disruption and muscle-fiber breakdown compared with control aphids (Fig. 3B-D; Fig. S7A,B).

TORC1-mediated nutritional signaling stimulates JH sensitivity in flight muscles

As shown above, JH sensitivity-induced flight-muscle degeneration depends on feeding (nutrition). The TORC1 pathway couples nutrition with JH biosynthesis in many insects (Maestro et al., 2009; Pérez-Hedo et al., 2013; Lu et al., 2016; Zhu et al., 2020). We then assessed whether TORC1 activity was also associated with nutrition-dependent JH sensitivity and flight-muscle degeneration in the process of the flight-reproduction life-history transition in aphids.

Limited by the efficiency of RNAi treatment, we used the TOR protein inhibitor rapamycin (Edwards and Wandless, 2007). About 60% of rapamycin-treated aphids died intensively by 72 h after the treatment (Fig. 3E). As expected, rapamycin reduced TORC1 activity in the whole body, excluding embryos, as evidenced by reduced 4EBP phosphorylation at 36, 60 and 72 h after the treatment (Fig. 3F). Rapamycin treatment specifically decreased the expression of *Met* and *Kr-h1* in the flight muscles, but had no effect on *JHAMT1-3* expression in the heads at 36 h after the treatment (Fig. 3G). By 60 h after rapamycin treatment, the effects of the TORC1 pathway could be observed in the regulation of JHAMT expression. The expression levels of *JHAMT2* in the heads of rapamycin-treated aphids were significantly downregulated at this time point (Fig. 3H), by which most flight muscles of the control aphids, which were already in larviposition mode, had degenerated. TEM analysis further showed that rapamycin treatment significantly inhibited flight-muscle degeneration, whereas methoprene application to rapamycin-treated aphids rescued *Kr-h1* expression and flight-muscle degeneration by 48 h after the treatment (Fig. 3I-M; Fig. S8A-C). Thus, TORC1-mediated nutritional signaling promotes JH sensitivity and signaling in the flight muscles, and causes muscle degeneration.

Development (2022) 149, dev200891. doi:10.1242/dev.200891

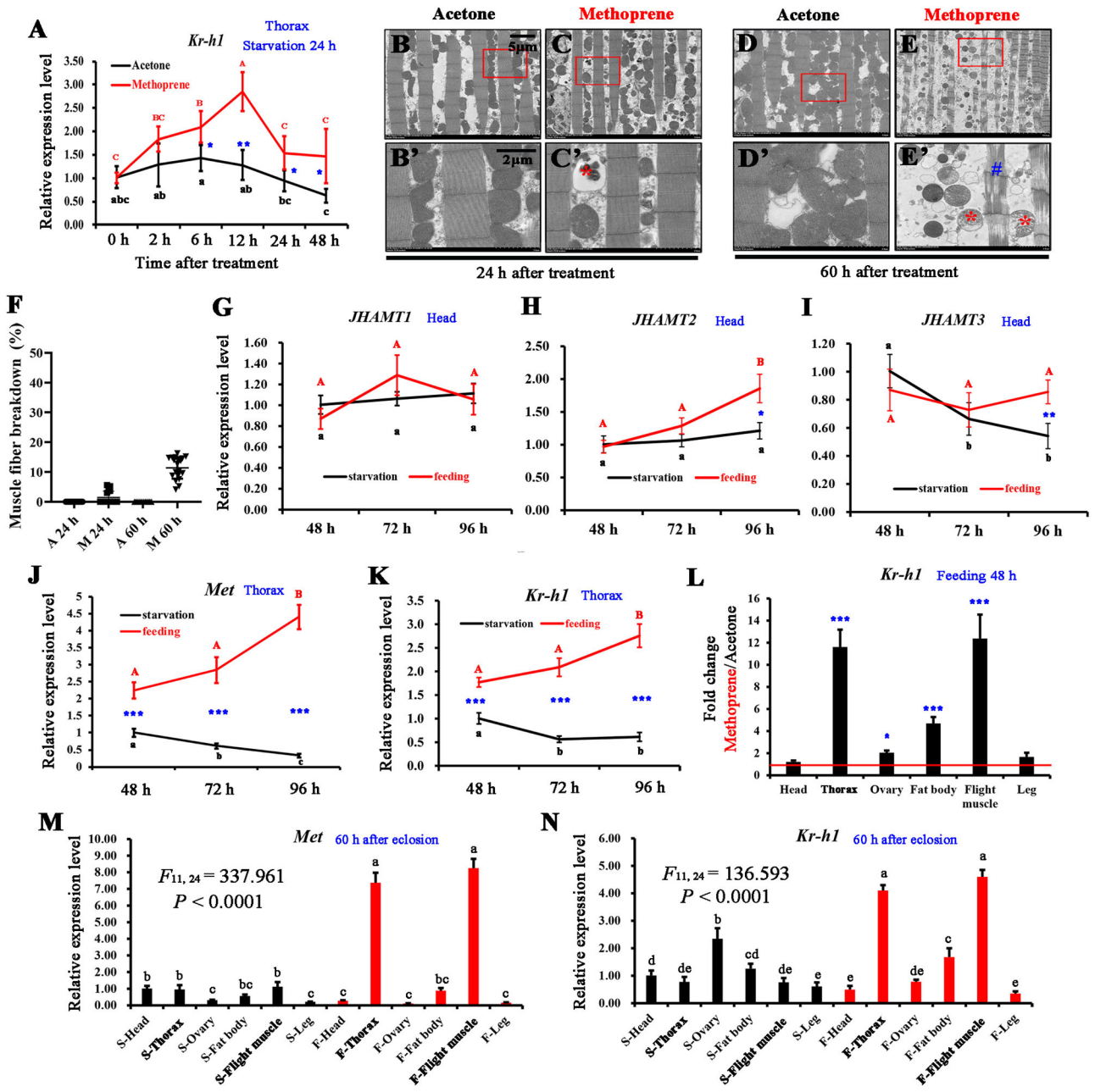

Fig. 2. Feeding stimulates tissue-specific JH sensitivity and signaling in the flight muscles of winged *A. pisum*. (A) Effect of methoprene application (100 ng/aphid) on *Kr-h1* expression in the thoraxes under the starvation condition. Methoprene was applied at 24 h post eclosion and the thoraxes were dissected at various time points after the treatment for qPCR analysis. The data are presented as the mean±s.e.m. from three biological replicates, and each replicate contained ten aphids. Two-tailed, unpaired Student's *t*-test was used to compare the differences between starvation and feeding groups at the same time point (**P*<0.05, ***P*<0.01). Different letters indicate statistically significant differences between various time points within starvation or feeding group using LSD multiple comparisons (*P*<0.05). (B-E) TEM images of the flight muscles at 24 and 60 h post methoprene treatment under the starvation condition. Muscle fibers and mitochondria in the red boxes in panels B-E are magnified in B′-E′ to show the degeneration of mitochondria (red asterisk) and muscle fibers (blue hash). *n*=5 for A 24 h, 10 for M 24 h, 5 for A 60 h, and 10 for M 60 h (A, acetone; M, methoprene). Eight and seven of the aphids in methoprene treatment at 24 and 60 h, respectively, displayed these degeneration characteristics. Other TEM samples with representative phenotypes for each group are shown in Fig. S4A-D. Scale bars: 5 µm (B-E); 2 µm (B′-E′). (F) Quantitative statistics of muscle fiber breakdown, shown as the percentage of 'blank muscle fiber area' to the total muscle fiber area; two or three images of each available TEM sample were selected for the area statistics, data are indicated as mean±s.e.m. (G-K) Transcriptional dynamics of *JHAMT1* (G), *JHAMT2* (H) and *JHAMT3* (I) in the heads, *Met* (J) and *Kr-h1* (K) in the thoraxes of fed and starved aphids at 48-96 h post eclosion. (L) Effect of methoprene application (100 ng/aphid) on *Kr-h1* expression in different body parts or tissues of the fed aphids. Methoprene was applied at 48 h post eclosion, and the tissues were dissected at 12 h after the treatment for qPCR analysis. (M-N) Relative expression levels of *Met* (M) and *Kr-h1* (N) in different body parts or tissues of fed ('F') and starved ('S') aphids at 60 h post eclosion. The qPCR data are presented as the mean±s.e.m. for three biological replicates (each replicate contains 10 aphids for the thoraxes or flight muscles, 30 aphids for the heads, 10 aphids for the ovaries, 20 aphids for the fat body and 50 aphids for the legs). The differences between the two groups were determined by two-tailed, unpaired Student's *t*-test (**P*<0.05, ***P*<0.01, ****P*<0.001), and differences among three or more groups were determined by LSD multiple comparisons (significant differences are indicated with different letters, *P*<0.05). *F* indicates the F-value (mean variances between groups/mean variances within groups, degree of freedom between groups=11, degree of freedom within groups=24) of variance significance F-test.

Development (2022) 149, dev200891. doi:10.1242/dev.200891

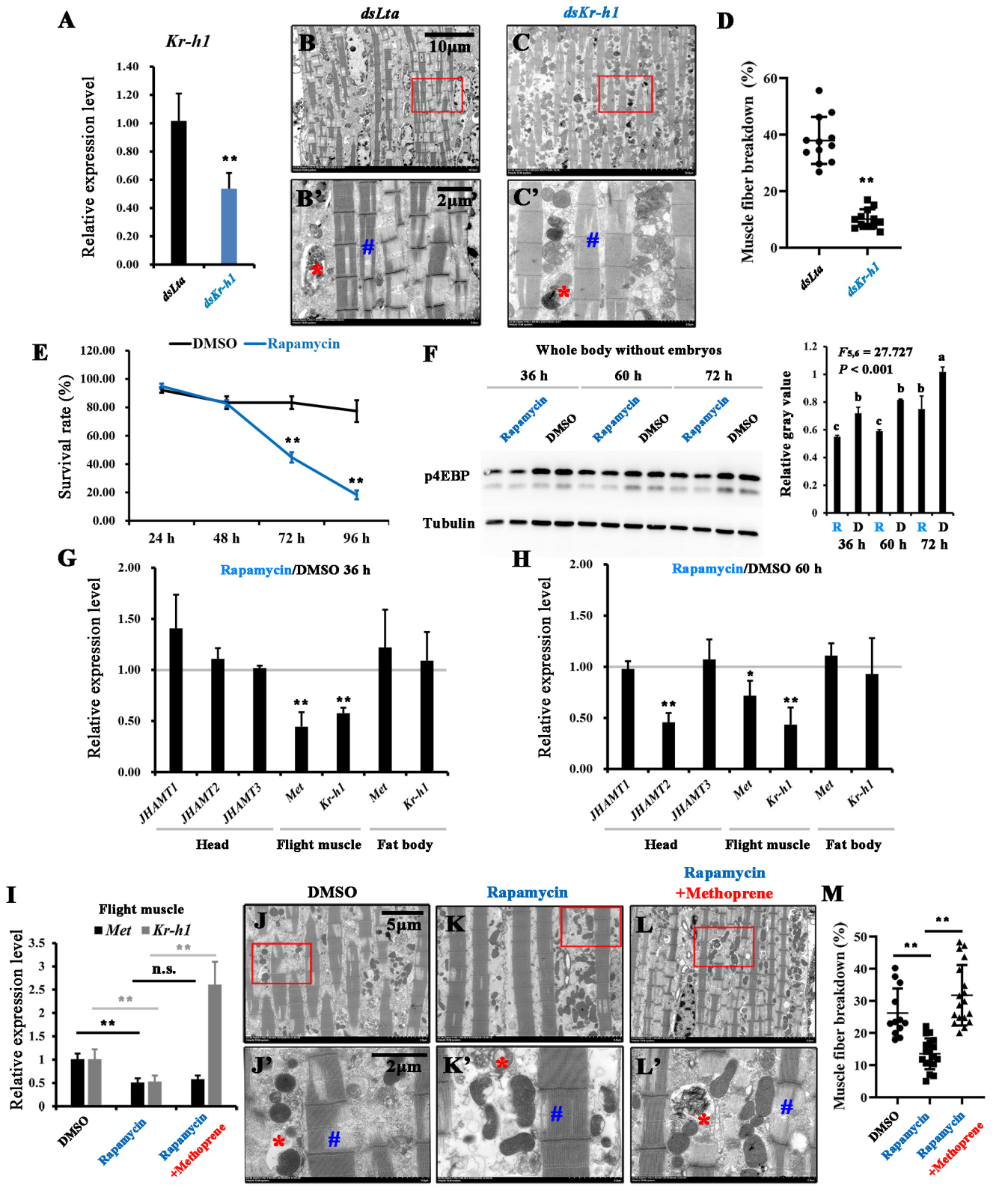

Fig. 3. See next page for legend.

Feeding and JH application suppress the TCA cycle and activate the proteasome pathway in flight muscles

We conducted two parallel RNA-seq experiments to further explore the molecular mechanism of JH-induced flight-muscle degeneration. In the two groups of experiments, JH signals were activated either by feeding or by artificial JH application in starvation (Fig. 4A,D). Principal component analysis (PCA) results showed high consistency between biological replicates of each treatment (Fig. S9A). RNA-seq analysis of the flight muscles identified 5160 differentially expressed genes between 'flight'- and

Development (2022) 149, dev200891. doi:10.1242/dev.200891

Fig. 3. TORC1 pathway-dependent JH sensitivity and signaling induces flight-muscle degeneration in winged *A. pisum*. (A) Effect of *Kr-h1* RNAi knockdown on *Kr-h1* transcripts. Injection of dsRNA was performed at 24 h after eclosion, and the flight muscles were dissected 48 h post injection for qPCR detection. (B,C) TEM observation of the flight muscles of *dsLta*- and *dsKr-h1*-injected aphids at 48 h after dsRNA injection. Detailed magnifications of the muscle fibers and mitochondria in B and C (red boxes) are shown in B′ and C′, respectively. Red asterisks and blue hashes indicate mitochondrial disruption and disrupted muscle fibers, respectively. (D) Quantitative evaluation of the degree of breakdown of muscle fibers, shown as the percentage of 'blank muscle fiber area' to the total muscle fiber area; data are indicated as mean±s.e.m.. Ten aphids were examined in each treatment, two or three images of each available TEM sample were selected for the area statistics. About 50% of the aphids with dsKr-h1 treatment display representative characteristics. Other TEM samples with representative phenotypes for each treatment are presented in Fig. S7E,F. (E) Survival rates (calculated for at least 90 aphids) of rapamycin- ('R') and DMSO- ('D') treated aphids during 24-96 h after the treatment, shown as mean±s.e.m. from three biological replicates. ***P*<0.01 (two-tailed, unpaired Student's *t*-test). (F-H) Effect of rapamycin treatment on phosphorylation levels of 4EBP at 36, 60 and 72 h after the treatment (F) and mRNA levels of *JHAMT1*, *JHAMT2*, *JHAMT3*, *Met* and *Kr-h1* at 36 h (G) and 60 h (H) after the treatment. Total proteins extracted from the whole body without embryos were used for western blot analysis. The heads were dissected for analyses of the expression of JHAMTs. The flight muscles and fat body were dissected for qPCR analyses of the JH signaling genes, *Met* and *Kr-h1*. *F* indicates the F-value (mean variances between groups/mean variances within groups, degree of freedom between groups=5, degree of freedom within groups=6) of variance significance F-test. (I) Response of the *Met* and *Kr-h1* transcript to methoprene application following rapamycin injection at 48 h post treatment. Injection of rapamycin (2 nM, 100 nl) and methoprene (1 mg/ml, 100 nl) application were performed 24 h post eclosion. All qPCR data are presented as the mean ±s.e.m. from three biological replicates. n.s., not significant; **P*<0.05; ***P*<0.01 (two-tailed, unpaired Student's *t*-test). (J-L) Histological changes of the flight muscles from DMSO-treated (J), rapamycin-treated (K), and methoprene-rescued (L) aphids at 48 h after the treatment. Detailed magnifications of muscle fibers and mitochondria in J-L (red boxes) are shown in J′-L′. Red asterisks and blue hashes indicate mitochondrial disruption and disrupted muscle fibers, respectively. (M) Quantitative statistics of muscle fiber breakdown, shown as the percentage of 'blank muscle fiber area' to the total muscle fiber area (*n*=5 for DMSO, 10 for rapamycin and 10 for rapamycin+methoprene); two or three images of each available TEM sample were selected for the area statistics, data are indicated as mean±s.e.m. ***P*<0.01 (two-tailed, unpaired Student's *t*-test). About 60% of the chemical-treated aphids display representative characteristics. Other TEM samples with representative phenotypes for each group are presented in Fig. S8.

'colonization'-mode females (Fig. 4B); the top pathways enriched in the KEGG aggregation analysis are listed in Table S4. A number of genes that are involved in the proteasome, protein processing and export, autophagy and the phagosome pathway were significantly upregulated, whereas other genes that regulate the citrate cycle (tricarboxylic acid or TCA cycle) of 2-oxocarboxylic acid or carbohydrate metabolism and oxidative phosphorylation, which are mainly responsible for releasing energy (ATP), were significantly downregulated in the females in 'colonization' mode compared with the females in 'flight' mode (Fig. 4C,H). The expression levels of seven of the differentially expressed genes involved in the TCA cycle were further validated by qPCR (Fig. S9B).

A total of 1282 genes were differentially expressed in the flight muscles between methoprene-treated and control females at 24 h after the treatment (Fig. 4E). KEGG aggregation analysis revealed the significantly upregulated and downregulated pathways (Table S5), which again included a number of genes with functions in the proteasome, in protein processing and export, and in the autophagy pathway that were significantly upregulated, whereas other genes involved in 2-oxocarboxylic acid metabolism in the TCA cycle were significantly downregulated in the flight muscles of methoprene-treated females compared with those in the acetone-treated females (Fig. 4F,H; Fig. S9C). In addition, heatCluster analysis of the 6442 differentially expressed genes showed that JH application and feeding resulted in almost consistent transcriptional changes in the flight muscles (Fig. 4G). RNA-seq experiments indicated that JH signaling inhibited the energy supply in the flight muscles of winged aphids. We then determined that the ATP levels in the flight muscles remained almost stable from 24 to 72 h post eclosion in starved aphids, whereas they were decreased upon feeding and JH application (Fig. 4I,J), which could contribute to flight-muscle degeneration. In conclusion, nutrition-dependent JH sensitivity promotes flight-muscle degeneration by suppressing the ATP supply and activating the expression of genes involved in the proteasome pathway in the flight muscles during the dispersal-reproduction transition in aphids.

DISCUSSION

First, this study emphasizes hormone sensitivity as a key regulatory mechanism of developmental events in insects. Hormone sensitivity usually refers to the expression levels of the hormone receptor and its associated proteins, as well as to the ability to respond to a hormone in a target tissue (Tang et al., 2011). During the colonization of winged aphids, nutrition-dependent gene expression levels of the JH nuclear receptor *Met*, an indicator of JH sensitivity, were quickly upregulated in the flight muscles; this upregulation initiates flight-muscle degeneration. Here, we demonstrate that TORC1-mediated nutritional signaling preferentially upregulates the expression of *Met*, leading to a tissue-specific increase of JH signaling (indicated by *Kr-h1* expression) in the flight muscles (Figs 1–3). The variation in hormone sensitivity between tissues could be a general regulatory mechanism underlying tissue-specific responses to hormones. Shingleton et al. (2005) also observed organ-specific sensitivity to insulin receptor signaling during development in *Drosophila*. Another example is the extreme growth of beetle horns, which are highly sensitive to changes in nutrition via insulin signaling (Emlen et al., 2012) and to sex differentiation via JH signaling (Gotoh et al., 2014). It is known that TORC1-mediated nutritional signaling plays roles in the stimulation of JH biosynthesis (Maestro et al., 2009; Pérez-Hedo et al., 2013; Lu et al., 2016; Zhu et al., 2020). There was no significant upregulation in any of the JH-biosynthesis genes at the beginning of flight-muscle degeneration. The *JHAMT* gene has been replicated in the pea aphid genome, but only *JHAMT2* was found to be regulated by the TORC1 pathway during larviposition mode (Fig. 3). In addition, the gene expression level of *JHAMT2* was the highest among the JHAMT genes, and *JHAMT2* was expressed in the heads in a tissue-specific manner (Fig. S6A). Thus, we deduce that the *JHAMT2* homolog is the functional JHAMT gene in the pea aphid. Nevertheless, in response to nutrition availability during the dispersal-reproduction transition of winged pea aphids, JH sensitivity in the flight muscles certainly plays a more important role than JH biosynthesis for flight-muscle degeneration.

Second, this study proves that JH promotes the dispersal-reproduction life-history transition of female winged aphids (Fig. 2). In addition to the experimental data presented, it has been shown that blocking JH biosynthesis with precocene II activates flight behavior (Kobayashi and Ishikawa, 1994); most of the precocene II-treated aphids flew away from the host plants and did not show any feeding behavior; thus, they did not undergo flight-muscle degeneration (Fig. S6B,C). Nevertheless, stable JH biosynthesis is necessary for colonization behavior and the subsequent dispersal-reproduction transition of winged aphids. JH

Development (2022) 149, dev200891. doi:10.1242/dev.200891

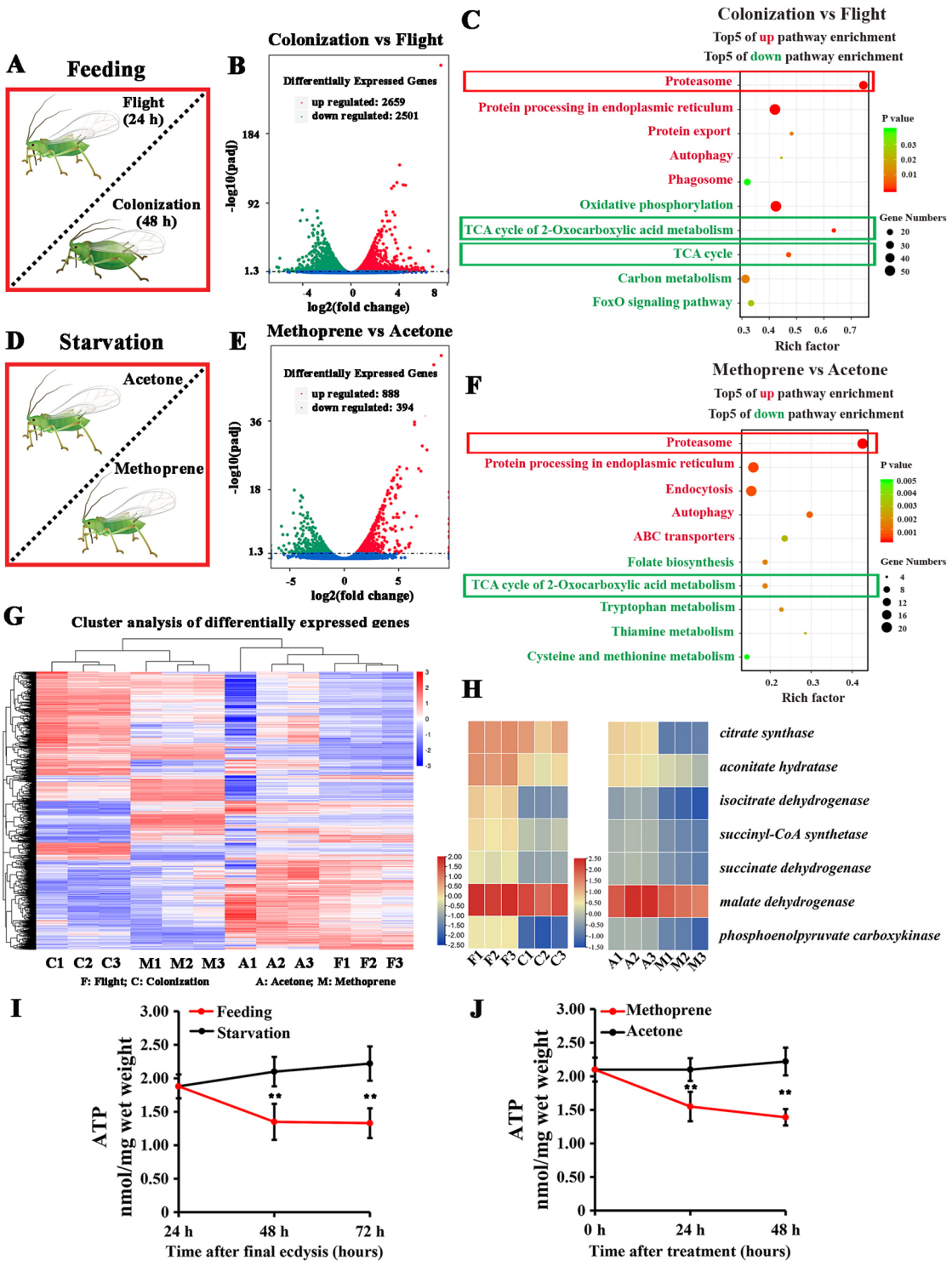

Fig. 4. Comparison of transcriptomes from flight muscles of control, feeding and exogenous JH mimic-treated winged aphids. (A-F) RNA-seq was performed based on two parallel experimental designs: the flight muscles of winged aphids in 'colonization' versus 'flight' mode (A) and the flight muscles of methoprene- versus acetone-treated aphids under starvation conditions (D) were sampled 24 h after treatment for comparative RNA-seq analysis. Newly collected aphids were subjected to 24 h of fasting prior to methoprene application (100 ng/aphid). Three independent biological samples (30 aphids were pooled to generate one biological replicate) were used for each experimental group to conduct differential expression analysis, and to produce the volcano plots (B,E). Adjusted *P*-values (P_{adj}, false discovery rate, FDR) were calculated using the Benjamini–Hochberg method. KEGG enrichment of functional and signaling pathways with respect to upregulated (red) and downregulated (green) gene sets generated from 'colonization' versus 'flight' (C) and 'methoprene' versus 'acetone' (F) differential expression analysis. (G,H) Heat maps represent the global transcriptional scenery of all differentially expressed genes (G) and the genes involved in the TCA cycle (H) in the flight muscles of 'colonization', 'flight', 'methoprene' and 'acetone' aphids. (I) Temporal dynamics of ATP levels in the flight muscles of fed and starved aphids from 24 to 72 h post eclosion. (J) Effect of methoprene application on ATP levels in the flight muscles of aphids under starvation conditions. Data are shown as mean±s.e.m. from three biological replicates, and each replicate contained 30 aphids. ***P*<0.01 (two-tailed, unpaired Student's *t*-test).

Development (2022) 149, dev200891. doi:10.1242/dev.200891

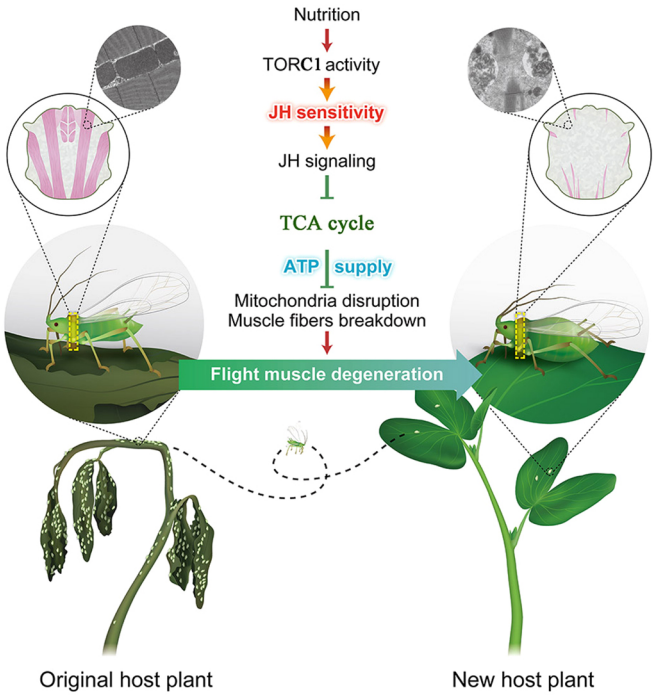

Fig. 5. Schematic diagram of the regulation mechanism underlying flight-muscle degeneration in winged *A. pisum*. The TORC1 pathway preferentially enhances JH sensitivity in the flight muscles, and the enhanced JH signaling blocks ATP supply via inhibition of the TCA cycle. A shortage of the energy supply most likely results in both mitochondrial disruption and muscle fiber breakdown, which contribute to the eventual degeneration of the flight muscles in winged aphids.

has been the main subject of endocrine regulation of dispersal-reproduction transitions in diverse insect species (Zhang et al., 2019). In response to environmental cues, such as nutrition availability, insects possess the ability to maintain metabolic homeostasis (Koyama et al., 2013; Johnson et al., 2014; Li et al., 2019b). Increasing evidence indicates that JH plays essential roles in the regulatory network of energy metabolism, with diverse and even opposing roles, depending on the developmental stage or physiological process in different insect species (Tian et al., 2010; Xu et al., 2013; Hou et al., 2015; Wang et al., 2017). Both dispersal and reproduction are costly, and loss of flight in stable habitats with available nutrition allows parthenogenetic winged aphids to shift resources toward the production of offspring away from flight. The combined data in this study suggest that a JH-induced tissue-specific reduction in energy supply mediates this transition in aphids (Fig. 4). It is worth mentioning that the mechanisms underlying the loss of flight are very different in male pea aphids, in which the wing dimorphisms are under genetic control (Li et al., 2020), and parthenogenetic females. The cricket *Gryllus firmus* should be an ideal model to verify whether the molecular mechanism that we discovered in the pea aphid is conserved in the regulation of flight-muscle degeneration in other insect species (Vellichirammal et al., 2014) and, moreover, to overcome the limitation of the low-efficiency of RNAi in the pea aphid.

Third, this study reveals that mitochondria might function as an important target organelle of JH signaling in the target tissue cells. Mitochondria are the primary energy-generating system in most eukaryotic cells. Mitochondrial dysfunction has pleiotropic effects on disease, aging and development (Chan, 2006). In almost all TEM analyses, we observed malformed mitochondria and mitochondrial matrix condensation, which precedes muscle-fiber breakdown (Figs 1-3). Notably, mitochondrial pathology is also a major causative factor for the earliest manifestation of muscle degeneration, as well as for muscle degeneration in Parkinson's disease (Greene et al., 2003). Impairment of the α-ketoglutarate dehydrogenase complex of the TCA cycle and respiratory chain complex I of the respiratory chain induces a decrease in ATP production and oxidative stress (Berndt et al., 2013), which could decrease the mitochondrial DNA content and trigger mitochondrial disruption, thus triggering apoptosis (Jaiswal et al., 2015; Tait and Green, 2010). Transcriptome analysis showed that JH suppresses gene expression in the TCA cycle pathway (Fig. 4), which might result in mitochondrial disruption and subsequent muscle-fiber breakdown. We have only partially verified this hypothesis using inhibitors of the TCA cycle and oxidative phosphorylation; these experiments are limited by the strong toxicity of systemic application of these chemicals.

In summary, TORC1-mediated nutritional signaling promotes JH sensitivity and thus JH signaling specifically in the flight muscles of winged aphids. The increased JH signaling inhibits the TCA cycle to reduce the energy supply and activates the expression of genes involved in the proteasome pathway, resulting in mitochondrial disruption and muscle-fiber breakdown in the flight muscles (Fig. 5). This study highlights that tissue-specific hormone sensitivity is an important regulatory mechanism of developmental transitions in insect life history.

MATERIALS AND METHODS

Insects and experimental apparatus

Wingless morphs of the pea aphid, *Acyrthosiphon pisum*, derived from a long-established parthenogenetic clone, were kept at low density. The aphids were maintained on broad bean seedlings in a climate chamber at 18°C and ∼70% relative humidity with a 16 h:8 h (light:dark) photoperiod. Winged morphs were induced under high-density conditions as described by Guo et al. (2016). The offspring produced during a 24 h period were retained and further screened on the basis of visible wing primordia at the third instar stage. Newly emerged adults within 12 h were collected to harvest winged aphids with synchronized development as described by Kobayashi and Ishikawa (1994). In the case of starvation, winged aphids were cultured in a Petri dish containing filter paper. In the case of feeding, newly emerged or treated winged aphids were cultured within our experimental cages for colonization (Fig. S10A).

Annotation and orthologue identification of JH pathway genes

To search for pea aphid orthologues of JH-related genes involved in biosynthesis and signaling, we performed BLAST analysis (http://blast.ncbi.nlm.nih.gov/) using the protein sequences of JH-related genes of *Drosophila melanogaster* with the *A. pisum* genome. The sequences with significantly lower E-values or those predicted by automated computational analysis as presupposed genes were chosen as the putative pea aphid orthologues (*HMGS1*, hydroxymethylglutaryl-CoA synthase 1, gene ID 100165154; *HMGS2*, hydroxymethylglutaryl-CoA synthase 2, gene ID 100161670; *HMGR*, 3-hydroxy-3-methylglutaryl-coenzyme A reductase, gene ID 100165462; *MVD*, diphosphomevalonate decarboxylase, gene ID 100574505; *IPPI*, isopentenyl diphosphate isomerase, gene ID 100166744; *FALD*, farnesol dehydrogenase, gene ID 100160714; *JHAMT1*, juvenile hormone acid O-methyltransferase, gene ID 100569254; *JHAMT2*, juvenile hormone acid O-methyltransferase-like, gene ID 100160278; *JHAMT3*, juvenile hormone acid methyltransferase, gene ID 100166857; *JHAMT4*, juvenile hormone acid O-methyltransferase-like, gene ID 100572117; *CYP15A1*, methyl farnesoate epoxidase-like, gene ID 100162751; *Met*, circadian locomoter output cycles protein kaput, gene ID 100573780; *Kr-h1*, zinc finger X-linked protein ZXDB, gene ID 100159203). RNA-seq analysis of the heads was employed to further estimate the functional *JHAMT* homolog in the pea aphid. The candidate

Development (2022) 149, dev200891. doi:10.1242/dev.200891

genes *Met* and *Kr-h1* were further verified by RT (reverse transcription)-PCR and re-sequencing. Briefly, the first-strand cDNA was synthesized using the PrimeScript II 1st Strand cDNA Synthesis Kit (Takara, Dalian, China). Target-specific primers (Table S1) were synthesized to amplify the complete coding sequences (CDSs) using the first-strand cDNA as templates, and high-fidelity PrimeSTAR GXL DNA Polymerase (Takara, Dalian, China) was used in our amplification experiments according to the manufacturer's protocol. PCR-amplified fragments were directly purified and supplied for sequencing. The ORF Finder (http://www.bioinformatics.org/sms2/orffind.html) was used to predict open reading frames, and the online tools ExPASy (https://web.expasy.org/translate/) and SMART (http://smart.embl-heidelberg.de) were used to translate and identify conserved functional domains based on our resequencing results, respectively (Fig. S10B,C). The sequenced complete CDSs of *Met-A* (OM371056), *Met-B* (OM371057), *Kr-h1-A* (OM371058) and *Kr-h1-B* (OM371059) were uploaded to the National Center for Biotechnology Information (NCBI) database. In addition, we performed RNAi against *Kr-h1* at the nymph stage of the pea aphid to further validate *Kr-h1* orthology. RNAi against *Kr-h1* at the third nymph stage resulted in abnormal wings post eclosion but no pre-metamorphosis phenotype (Fig. S10D).

Chemicals, topical application and microinjection

The JH mimic methoprene (Sigma-Aldrich), the corpus allatum inhibitor precocene II (Yuanye Bio-Technology, Shanghai, China) and the TOR inhibitor rapamycin (Selleck, Shanghai, China) were used in this study. Methoprene (1 mg/ml) and precocene II (50 mg/ml) solutions were prepared with acetone, and 100 nl of the solution was topically applied to the aphid pronotum using a Nanoject II injector (Drummond Scientific). The aphids in flight mode were treated with methoprene, and the treated aphids were subjected to starvation or feeding for JH induction or rescue experiment, respectively; methoprene application on the femur served as a parallel control of JH induction experiment. Besides, the aphids in colonization mode were treated with methoprene and the treated aphids were subjected to feeding for another JH induction experiment. Rapamycin was first dissolved in DMSO and further diluted to 2 nM with 0.01 M PBS, and 100 nl of the solution was delivered into the abdomen via microinjection. The aphids in flight mode were treated with rapamycin or precocene II using the Nanoject II injector, and the aphids were placed in the feeding cages after the treatment. At least 30 aphids were treated for each group every time.

qPCR and RNA sequencing

qPCR was employed to detect the changes in JH biosynthesis and signaling levels during *A. pisum* winged adult colonization or after chemical or RNAi treatment. The spatial expression profiles of *Met* and *Kr-h1* were determined using tissues from the heads (30 individuals for one biological replicate), thoraxes (10 individuals), ovaries (10 individuals), fat body (20 individuals), flight muscles (10 individuals) and legs (50 individuals) of winged adults at feeding or starvation 60 h after eclosion. The temporal expression profiles of JHAMTs, *Met* and *Kr-h1* at different developmental stages of winged adults subjected to feeding or starvation conditions post eclosion were determined using head samples for JHAMTs and thorax samples for *Met* and *Kr-h1*. For the topical application of methoprene, starved winged aphids were treated at 24 h post eclosion and the thoraxes were excised from the specimen at 2, 6, 12, 24 and 48 h after the treatment; whereas feeding winged aphids were treated 48 h post eclosion and the heads, thoraxes, ovaries, fat body, flight muscles and legs were excised from the specimens 12 h after the treatment for qPCR analysis. For RNAi and rapamycin application experiments, the heads were excised for JHAMT detection and the flight muscles or fat body were excised for *Met* and *Kr-h1* detection at specific points in time. Three independent biological replicates were performed in all qPCR analyses. All of the samples were stored in RNAiso Plus (Takara) at −80°C until use. Following total RNA isolation and reverse transcription, qPCR was performed on an IQ-5 Real-time system (Bio-Rad). The expression levels of *A. pisum* elongation factor 1 α (*EF1a*) and ribosomal protein S20 (*Rps20*) were quantified as housekeeping genes for normalization (Chen et al., 2016; Ishikawa et al., 2012). The cycle threshold values normalized against the means of *EF1a* and *Rps20* standard values were obtained to calculate the quantitative variation of target genes using the mathematical model by Pfaffl (2001) and the REST 2009 software (QIAGEN). Gene-specific qPCR primers (targeting the common regions of transcript variants) with appropriate amplification efficiency were screened by cDNA gradient-based standard curves (Table S2).

Four groups of flight-muscle samples and two groups of head samples (each group containing three independent biological replicates) were prepared for RNA sequencing. In the feeding condition, winged adults in 'flight' and 'colonization' modes were subjected to flight-muscle (48 h post eclosion) or head (60 h post eclosion) sampling. In the starvation condition, acetone- and methoprene-treated aphids were subjected to flight-muscle sampling at 24 h after the treatment. Each flight-muscle or head sample was collected from at least 30 aphids and was prepared for RNA extraction. An aliquot of 1000 ng of total mRNA from each sample was used to construct libraries. Single-end, 1×50 sequencing was performed on an Illumina HiSeq 2500 at the Novogene sequencing facility (Beijing, China). The genome sequence and annotation files of *A. pisum* were downloaded from the NCBI database (https://www.ncbi.nlm.nih.gov/genome/?term=pea+aphid). The clean reads were mapped to the genome using genomic short-read nucleotide alignment program (GSNAP) to estimate the expression level of all transcripts (Wu et al., 2005). Gene expression levels were estimated by fragments per kilobase of transcript per million fragments mapped. Differential expression analysis of two groups was performed using the DESeq R package (1.10.1). Genes with an adjusted *P*-value (false discovery rate, FDR)<0.05 found by DESeq were designated as differentially expressed. We used KOBAS (Mao et al., 2005) software to test the statistical enrichment of differentially expressed genes in KEGG pathways. The entire RNA-seq datasets are available online (PRJNA828046).

RNAi experiments

Gene-specific primers (Table S3) were designed to amplify a 307 bp fragment (common regions of isoforms A and B) for *Kr-h1*. A 193 bp fragment of the *Mus musculus* lymphotoxin A (*Lta*) was also cloned to serve as an unrelated control gene. The validated plasmid and primers containing T7 RNA polymerase promoter were subjected to PCR amplification to produce DNA templates used for double-stranded RNA (dsRNA) synthesis. DsRNA synthesis and purification were performed using a T7 RiboMAX Express RNAi System (Promega), according to the manufacturer's instructions. The concentration of the purified dsRNA was quantified at 260 nm using a NanoDrop 2000c spectrophotometer (Thermo Fisher Scientific), and was adjusted to 6 µg/µl with RNase-free water. Newly emerged aphids were subjected to 24 h of fasting prior to dsRNA microinjection. They were anesthetized with carbon dioxide, and 150 nl of specific dsRNA was injected into the aphid hemolymph using a Nanoject II injector. The dsRNA-treated aphids were placed in the feeding cages for colonization. At least 30 aphids were treated for each group every time.

Transmission electron microscopy

Newly collected muscle tissues were fixed in 2.5% glutaraldehyde at 4°C overnight followed by thorough washing with PBS. The specimens were then postfixed in 0.5% osmium tetroxide for 2 h, dehydrated in an ethanol gradient and finally embedded in Epon resin. Longitudinal sections (70 nm) of muscle fibers were prepared using a UC7 ultramicrotome (Leica), stained with Reynold's lead citrate and visualized on an HT7700 transmission electron microscope (Hitachi, Tokyo, Japan) to observe the degree of breakage of muscle fibers and the morphology of mitochondria. Quantitative analysis of the damaged muscle fibers was performed by ImageJ.

Western blot analysis

For each sample, 30 aphids without embryos were lysed directly for total protein extraction. Proteins were separated by 12% SDS-PAGE and transferred to a polyvinylidene fluoride membrane. The loaded membrane was then blocked with 5% bovine serum albumin in TBS supplemented with 1% Tween-20 (TBST, pH 8.0) for 1 h at room temperature and incubated with 1:1000 diluted primary antibodies (anti-phospho-4EBP, Thr37/46,

2855S, Cell Signaling Technology; and anti-tubulin, AF1216; Beyotime Biotechnology, China) at 4°C overnight. The primary antibodies specifically bind to target proteins. Then, the membrane was incubated with goat anti-rabbit IgG-HRP secondary antibody (1:5000; A0181, Beyotime Biotechnology) for 1 h at room temperature. The immune signal was visualized by the ECL chemiluminescent substrate (Boster, Wuhan, China), and images were captured on a ChemiDoc MP System (Bio-Rad). Quantitative analysis of the protein bands was performed by ImageJ.

ATP assay

ATP levels in the flight muscles were determined using an ATP Assay Kit (Fluorometric) (ab83355, Abcam). A standard curve was established from a pure ATP gradient according to the manufacturer's instructions. In each biological replicate, approximately 10 mg of the aphid thoraxes was homogenized in 2 N perchloric acid and the diluted supernatant was neutralized with 2 M KOH. These deproteinized samples and ATP reaction mixes were successively added into a black 96-well plate, and the reaction was incubated at room temperature for 30 min. The fluorescence readings were measured by an Infinite 200 microplate reader (Tecan, Männedorf, Switzerland) with the excitation/emission setting at 535/587 nm. The mean fluorescence intensity was determined by comparison to a standard curve.

Acknowledgements

The authors are grateful to Prof. Michael R. Strand (University of Georgia), Yun-Xia Luan (South China Normal University, China) and Dr He-He Cao (Northwest A&F University, China) for critical revision of the manuscript, and to the Sagene Biotech Co., Ltd. (Guangzhou, China) for the schematics of aphids and plants used in Fig. 5.

Competing interests

The authors declare no competing or financial interests.

Author contributions

Conceptualization: Y.B.; Methodology: Y.B., X.-J.P., N.C.; Validation: Y.B., X.-J.P.; Formal analysis: Y.B., N.B., N.C., S.-N.L.; Investigation: N.B.; Data curation: Y.B., N.B., S.-N.L.; Writing - original draft: Y.B.; Writing - review & editing: X.-J.P., N.C., S.-N.L., S.L., T.-X.L.; Supervision: S.L., T.-X.L.; Funding acquisition: S.L., T.-X.L.

Funding

This work was supported by the Special Talent Fund of the Northwest A and F University, the National Natural Science Foundation of China (31471819 and 31660522), National Basic Research Program of China (973 Program; 2013CB127600), and Agriculture Research System of China (CARS-25-B-06) grants to T.-X.L.; and the National Natural Science Foundation of China (31620103917) and the Shenzhen Science and Technology Innovation Program (20180411143628272) grants to S.L.

Data availability

The entire RNA-seq datasets of the flight muscle and head of *A. pisum* have been deposited in the NCBI database under the accession number PRJNA828046. The complete CDSs of *Met-A* (OM371056), *Met-B* (OM371057), *Kr-h1-A* (OM371058) and *Kr-h1-B* (OM371059) are also available in the NCBI database.

References

Beldade, P., Mateus, A. and Keller, R. (2011). Evolution and molecular mechanisms of adaptive developmental plasticity. *Mol. Ecol.* **20**, 1347-1363. doi:10.1111/j.1365-294X.2011.05016.x

Berndt, N., Holzhütter, H.-G. and Bulik, S. (2013). Implications of enzyme deficiencies on mitochondrial energy metabolism and reactive oxygen species formation of neurons involved in rotenone-induced Parkinson's disease: a model-based analysis. *FEBS J.* **280**, 5080-5093. doi:10.1111/febs.12480

Bonte, D., Van Dyck, H., Bullock, J. M., Coulon, A., Delgado, M. M., Gibbs, M., Lehouck, V., Matthysen, E., Mustin, K., Saastamoinen, M. et al. (2012). Costs of dispersal. *Biol. Rev.* **87**, 290-312. doi:10.1111/j.1469-185X.2011.00201.x

Brisson, J. A. (2010). Aphid wing dimorphisms: linking environmental and genetic control of trait variation. *Phil. Trans. R. Soc. B* **365**, 605-616. doi:10.1098/rstb.2009.0255

Chan, D. C. (2006). Mitochondria: dynamic organelles in disease, aging, and development. *Cell* **7**, 1241-1252. doi:10.1016/j.cell.2006.06.010

Chen, N., Fan, Y.-L., Bai, Y., Li, X.-D., Zhang, Z.-F. and Liu, T.-X. (2016). Cytochrome P450 gene, *CYP4G51*, modulates hydrocarbon production in the pea aphid, *Acyrthosiphon pisum*. *Insect Biochem. Mol. Biol.* **76**, 84-94. doi:10.1016/j.ibmb.2016.07.006

Colombani, J., Raisin, S., Pantalacci, S., Radimerski, T., Montagne, J. and Léopold, P. (2003). A nutrient sensor mechanism controls *Drosophila* growth. *Cell* **114**, 739-749. doi:10.1016/S0092-8674(03)00713-X

Edwards, S. R. and Wandless, T. J. (2007). The rapamycin-binding domain of the protein kinase mammalian target of rapamycin is a destabilizing domain. *J. Biol. Chem.* **4**, 13395-13401. doi:10.1074/jbc.M700498200

Emlen, D. J., Warren, I. A., Johns, A., Dworkin, I. and Lavine, L. C. (2012). A mechanism of extreme growth and reliable signaling in sexually selected ornaments and weapons. *Science* **337**, 860-864. doi:10.1126/science.1224286

Géminard, C., Rulifson, E. J. and Léopold, P. (2009). Remote control of insulin secretion by fat cells in Drosophila. *Cell Metab.* **10**, 199-207. doi:10.1016/j.cmet.2009.08.002

Gotoh, H., Miyakawa, H., Ishikawa, A., Ishikawa, Y., Sugime, Y., Emlen, D. J., Lavine, L. C. and Miura, T. (2014). Developmental link between sex and nutrition: doublesex regulates sex-specific mandible growth via juvenile hormone signaling in stag beetles. *PLoS Genet.* **10**, e1004098. doi:10.1371/journal.pgen.1004098

Greene, J. C., Whitworth, A. J., Kuo, I., Andrews, L. A., Feany, M. B. and Pallanck, L. J. (2003). Mitochondrial pathology and apoptotic muscle degeneration in *Drosophila* parkin mutants. *Proc. Natl. Acad. Sci. USA* **100**, 4078-4083. doi:10.1073/pnas.0737556100

Guerra, P. A. (2011). Evaluating the life-history trade-off between dispersal capability and reproduction in wing dimorphic insects: a meta-analysis. *Biol. Rev. Camb. Philos. Soc.* **86**, 813-835. doi:10.1111/j.1469-185X.2010.00172.x

Guo, S., Zhang, M. and Liu, T. X. (2016). Insulin-related peptide 5 is involved in regulating embryonic development and biochemical composition in pea aphids with wing ploiphenism. *Front. Physiol.* **7**, 31. doi:10.3389/fphys.2016.00031

Hietakangas, V. and Cohen, S. M. (2009). Regulation of tissue growth through nutrient sensing. *Annu. Rev. Genet.* **43**, 389-410. doi:10.1146/annurev-genet-102108-134815

Hou, Y., Wang, X.-L., Saha, T. T., Roy, S., Zhao, B., Raikhel, A. S. and Zou, Z. (2015). Temporal coordination of carbohydrate metabolism during mosquito reproduction. *PLoS Genet.* **11**, e1005309. doi:10.1371/journal.pgen.1005309

Howell, J. J. and Manning, B. D. (2011). mTOR couples cellular nutrient sensing to organismal metabolic homeostasis. *Trends Endocrin. Met.* **22**, 94-102. doi:10.1016/j.tem.2010.12.003

Ishikawa, A., Ogawa, K., Gotoh, H., Walsh, T. K., Tagu, D., Brisson, J. A., Rispe, C., Jaubert-Possamai, S., Kanbe, T., Tsubota, T. et al. (2012). Juvenile hormone titre and related gene expression during the change of reproductive modes in the pea aphid. *Insect Mol. Biol.* **21**, 49-60. doi:10.1111/j.1365-2583.2011.01111.x

Jaiswal, N., Maurya, C. K., Arha, D., Avisetti, D. R., Prathapan, A., Raj, P. S., Raghu, K. G., Kalivendi, S. V. and Tamrakar, A. K. (2015). Fructose induces mitochondrial dysfunction and triggers apoptosis in skeletal muscle cells by provoking oxidative stress. *Apoptosis* **20**, 930-947. doi:10.1007/s10495-015-1128-y

Jindra, M., Palli, S. R. and Riddiford, L. M. (2013). The juvenile hormone signaling pathway in insect development. *Annu. Rev. Entomol.* **58**, 181-204. doi:10.1146/annurev-ento-120811-153700

Johnson, B. (1959). Studies on the degeneration of the flight muscles of alate aphids: II histology and control of muscle breakdown. *J. Insect Physiol.* **3**, 367-377. doi:10.1016/0022-1910(59)90039-3

Johnson, E. C., Braco, J. T. and Whitmill, M. A. (2014). Connecting nutrient sensing and the endocrine control of metabolic allocation in insects. *Curr. Opin. Insect Sci.* **1**, 66-72. doi:10.1016/j.cois.2014.05.005

Kobayashi, M. and Ishikawa, H. (1993). Breakdown of indirect flight muscles of alate aphids (*Acyrthosiphon pisum*) in relation to their flight, feeding and reproductive behavior. *J. Insect Physiol.* **39**, 549-554. doi:10.1016/0022-1910(93)90036-Q

Kobayashi, M. and Ishikawa, H. (1994). Involvement of juvenile hormone and ubiquitin-dependent proteolysis in flight muscle breakdown of alate aphid (*Acyrthosiphon pisum*). *J. Insect Physiol.* **40**, 107-111. doi:10.1016/0022-1910(94)90081-7

Konopova, B. and Jindra, M. (2007). Juvenile hormone resistance gene Methoprene-tolerant controls entry into metamorphosis in the beetle *Tribolium castaneum*. *Proc. Natl. Acad. Sci. USA.* **104**, 10488-10493. doi:10.1073/pnas.0703719104

Koyama, T., Mendes, C. C. and Mirth, C. K. (2013). Mechanisms regulating nutrition-dependent developmental plasticity through organ-specific effects in insects. *Front. Physiol.* **4**: 263. doi:10.3389/fphys.2013.00263

Li, K., Jia, Q. Q. and Li, S. (2019a). Juvenile hormone signaling-a mini review. *Insect Sci.* **26**, 600-606. doi:10.1111/1744-7917.12614

Li, S., Yu, X. and Feng, Q. (2019b). Fat body biology in the last decade. *Annu. Rev. Entomol.* **64**, 315-333. doi:10.1146/annurev-ento-011118-112007

Li, B. S., Bickel, R. D., Parker, B. J., Ziabari, O. S., Liu, F. Z., Vellichirammal, N. N., Simon, J. C., Stern, D. L. and Brisson, J. A. (2020). A large genomic insertion containing a duplicated follistatin gene is linked to the pea aphid male wing dimorphism. *eLife*, **9**, e50608. doi:10.7554/eLife.50608

Lu, K., Chen, X., Liu, W.-T. and Zhou, Q. (2016). TOR pathway-mediated juvenile hormone synthesis regulates nutrient-dependent female reproduction in *Nilaparvata lugens* (Stål). *Int. J. Mol. Sci.* **17**, 438. doi:10.3390/ijms17040438

Maestro, J. L., Cobo, J. and Bellés, X. (2009). Target of rapamycin (TOR) mediates the transduction of nutritional signals into juvenile hormone production. *J. Biol. Chem.* **284**, 5506-5513. doi:10.1074/jbc.M807042200

Mao, X., Cai, T., Olyarchuk, J. G. and Wei, L. (2005). Automated genome annotation and pathway identification using the KEGG Orthology (KO) as a controlled vocabulary. *Bioinformatics* **21**, 3787-3793. doi:10.1093/bioinformatics/bti430

Miura, T. (2018). Juvenile hormone as a physiological regulator mediating phenotypic plasticity in Pancrustaceans. *Dev. Growth Differ.* **61**, 85-96. doi:10.1111/dgd.12572

Nijhout, H. F. (1999). Control mechanisms of polyphenic development in insects. *Bioscience* **49**, 181-192. doi:10.2307/1313508

Pérez-Hedo, M., Rivera-Perez, C. and Noriega, F. G. (2013). The insulin/TOR signal transduction pathway is involved in the nutritional regulation of juvenile hormone synthesis in *Aedes aegypti*. *Insect Biochem. Mol. Biol.* **43**, 495-500. doi:10.1016/j.ibmb.2013.03.008

Pfaffl, M. W. (2001). A new mathematical model for relative quantification in real-time RT-PCR. *Nucleic Acids Res.* **29**, e45. doi:10.1093/nar/29.9.e45

Reiff, T., Jacobson, J., Cognigni, P., Antonello, Z., Ballesta, E., Tan, K. J., Yew, J. Y., Dominguez, M. and Miguel-Aliaga, I. (2015). Endocrine remodelling of the adult intestine sustains reproduction in *Drosophila*. *eLife* **4**, e06930. doi:10.7554/eLife.06930

Roy, S., Saha, T. T., Zou, Z. and Raikhel, A. S. (2018). Regulatory pathways controlling female insect reproduction. *Annu. Rev. Entomol.* **63**, 489-511. doi:10.1146/annurev-ento-020117-043258

Shingleton, A. W., Das, J., Vinicius, L. and Stern, D. L. (2005). The temporal requirements for insulin signaling during development in *Drosophila*. *PLoS Biol.* **3**, e289. doi:10.1371/journal.pbio.0030289

Shinoda, T. and Itoyama, K. (2003). Juvenile hormone acid methyltransferase: A key regulatory enzyme for insect metamorphosis. *Proc. Natl. Acad. Sci. USA* **100**, 11986-11991. doi:10.1073/pnas.2134232100

Simpson, S. J., Sword, G. A. and Lo, N. (2011). Polyphenism in insects. *Curr. Biol.* **21**, 738-749. doi:10.1016/j.cub.2011.06.006

Tait, S. W. G. and Green, D. R. (2010). Mitochondria and cell death: outer membrane permeabilization and beyond. *Nature Rev. Mol. Cell Biol.* **11**, 621-632. doi:10.1038/nrm2952

Tang, H. Y., Smith-Caldas, M. S. B., Driscoll, M. V., Salhadar, S. and Shingleton, A. W. (2011). FOXO regulates organ-specific phenotypic plasticity in *Drosophila*. *PLoS Genet.* **7**, e1002373. doi:10.1371/journal.pgen.1002373

Tian, L., Guo, E., Wang, S., Liu, S., Jiang, R.-J., Cao, Y., Ling, E. and Li, S. (2010). Developmental regulation of glycolysis by 20-hydroxyecdysone and juvenile hormone in fat body tissues of the silkworm, *Bombyx mori*. *J. Mol. Cell Biol.* **2**, 255-263. doi:10.1093/jmcb/mjq020

Vellichirammal, N. N., Zera, A. J., Schilder, R. J., Wehrkamp, C., Riethoven, J.-J. M. and Brisson, J. A. (2014). De novo transcriptome assembly from fat body and flight muscles transcripts to identify morph-specific gene expression profiles in *Gryllus firmus*. *PLoS ONE* **9**, e82129. doi:10.1371/journal.pone.0082129

Wang, X., Hou, Y., Saha, T., Pei, G., Raikhel, A. and Zou, Z. (2017). Hormone and receptor interplay in the regulation of mosquito lipid metabolism. *Proc. Natl. Acad. Sci. USA* **114**, E2709-E2718. doi:10.1073/pnas.1619326114

Weigang, H. C. and Kisdi, E. (2015). Evolution of dispersal under a fecundity-dispersal trade-off. *J. Theor. Biol.* **371**, 145-153. doi:10.1016/j.jtbi.2015.02.013

Wen, D., Rivera-Perez, C., Abdou, M., Jia, Q., He, Q., Liu, X., Zyaan, O., Xu, J., Bendena, W. G., Tobe, S. S. et al. (2015). Methyl farnesoate plays a dual role in regulating *Drosophila* metamorphosis. *PLoS Genet.* **13**, e1006559. doi:10.1371/journal.pgen.1006559

Wu, T. D. and Watanabe, C. K. (2005). GMAP: a genomic mapping and alignment program for mRNA and EST sequences. *Bioinformatics* **21**, 1859-1875. doi:10.1093/bioinformatics/bti310

Xu, J., Sheng, Z. and Palli, S. R. (2013). Juvenile hormone and insulin regulate trehalose homeostasis in the red flour beetle, *Tribolium castaneum*. *PLoS Genet.* **9**, e1003535. doi:10.1371/journal.pgen.1003535

Zera, A. J. and Denno, R. F. (1997). Physiology and ecology of dispersal polymorphism in insects. *Annu. Rev. Entomol.* **42**, 207-230. doi:10.1146/annurev.ento.42.1.207

Zhang, C.-X., Brisson, J. A. and Xu, H.-J. (2019). Molecular mechanisms of wing polymorphism in insects. *Annu. Rev. Entomol.* **64**, 1-18. doi:10.1146/annurev-ento-011118-112448

Zhu, S. M., Liu, F. F., Zeng, H. C., Li, N., Ren, C. H., Su, Y. L., Zhou, S. T., Wang, G. R., Palli, S. R., Wang, J. et al. (2020). Insulin/IGF signaling and TORC1 promote vitellogenesis via inducing juvenile hormone biosynthesis in the American cockroach. *Development* **147**, dev188805. doi:10.1242/dev.188805

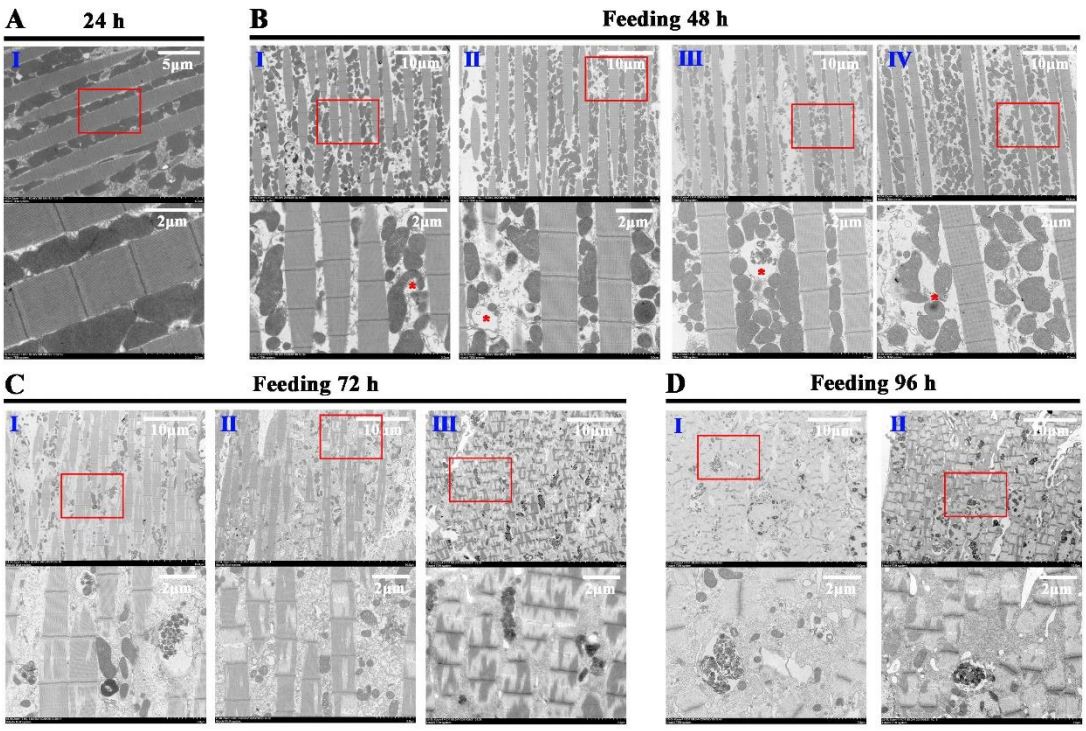

Fig. S1. Feeding induces flight muscle degeneration in winged female *A. pisum*. Transmission electron microscopy (TEM) observations of the flight muscles from 24 h to 96 h post eclosion under feeding conditions (A–D). Detailed magnifications of the sections in the red box highlighting muscle fibers and mitochondria below the corresponding picture. "*" indicates disrupted mitochondrial. I–IV represents biological replications.

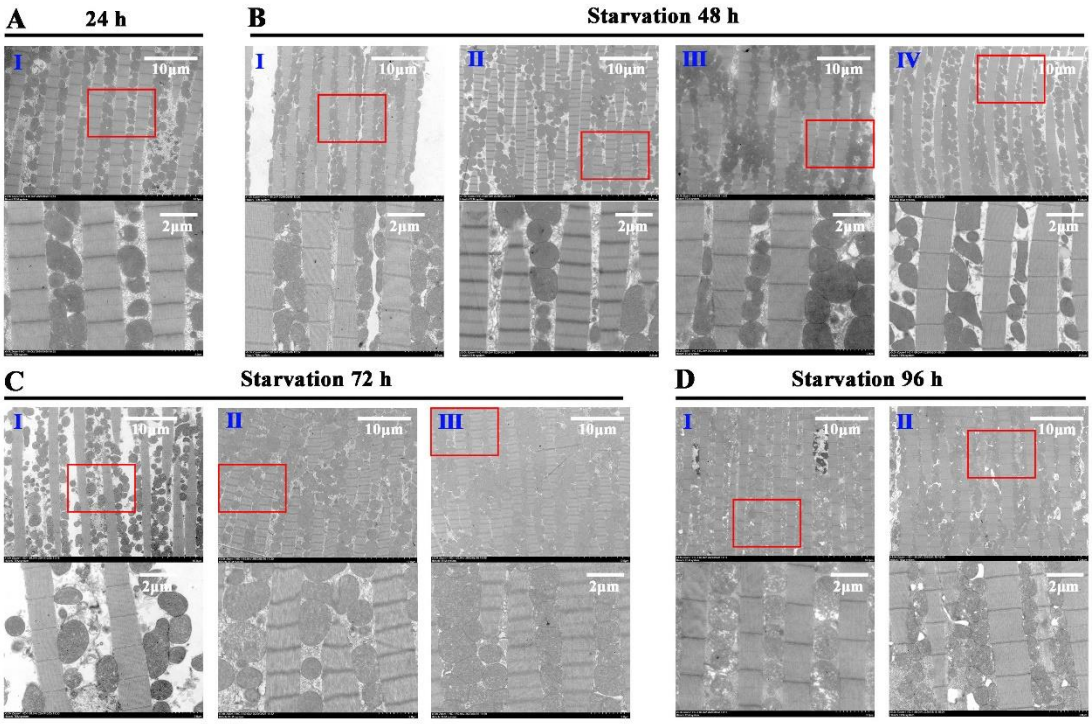

Fig. S2. Flight muscle degeneration would not occur during starvation post eclosion in winged female *A. pisum*. TEM observations of the flight muscles from 24 h to 96 h post eclosion under starvation (A–D). Detailed magnifications of the sections in the red box highlighting muscle fibers and mitochondria below the corresponding picture. I–IV represents biological replications.

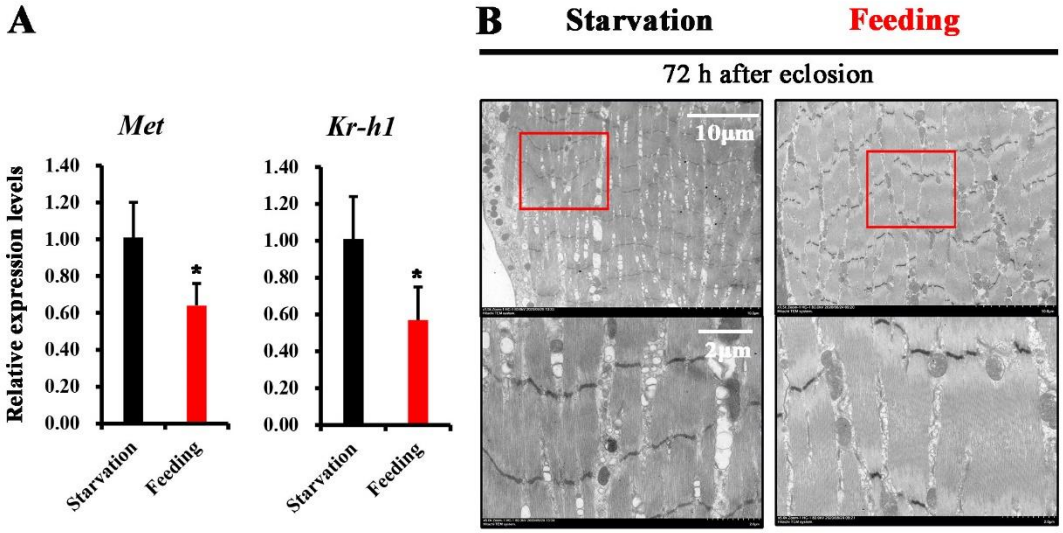

Fig. S3. Feeding-induced muscle degeneration would not occur in the leg muscles during winged aphid colonization. (A) Relative expression levels of *Met* and *Kr-h1* in the legs of fed and starved aphids at 72 h post eclosion. The data are presented as the mean ± s.e.m. from 3 biological replicates, and each replicate contains 50 aphids. Student's t-test was used to compare the differences between starvation and feeding groups (*$P < 0.05$). (B) Longitudinal ultrathin sections of leg muscles in winged female aphids under feeding 72 h and starvation 72 h post eclosion identified by TEM.

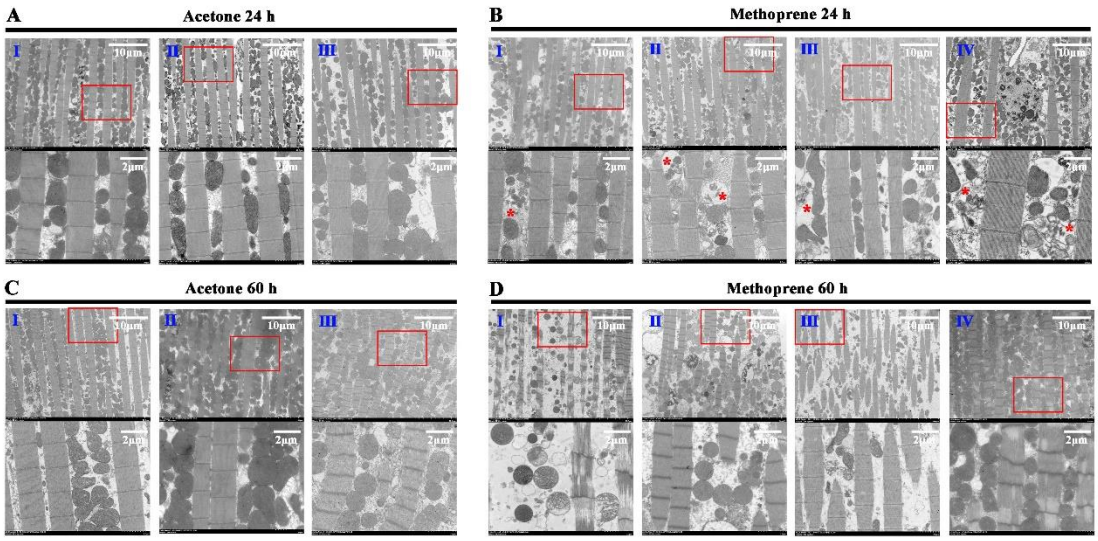

Fig. S4. JH application induces mitochondrial disruption and flight muscle fiber breakdown during starvation in winged female *A. pisum*. TEM observations of the flight muscles at 24 h (A and B) and 60 h (C and D) after methoprene treatment under starvation. Detailed magnifications of the sections in the red box highlighting muscle fibers and mitochondria below the corresponding picture. "*" indicates disrupted mitochondrial. I–IV represents biological replications.

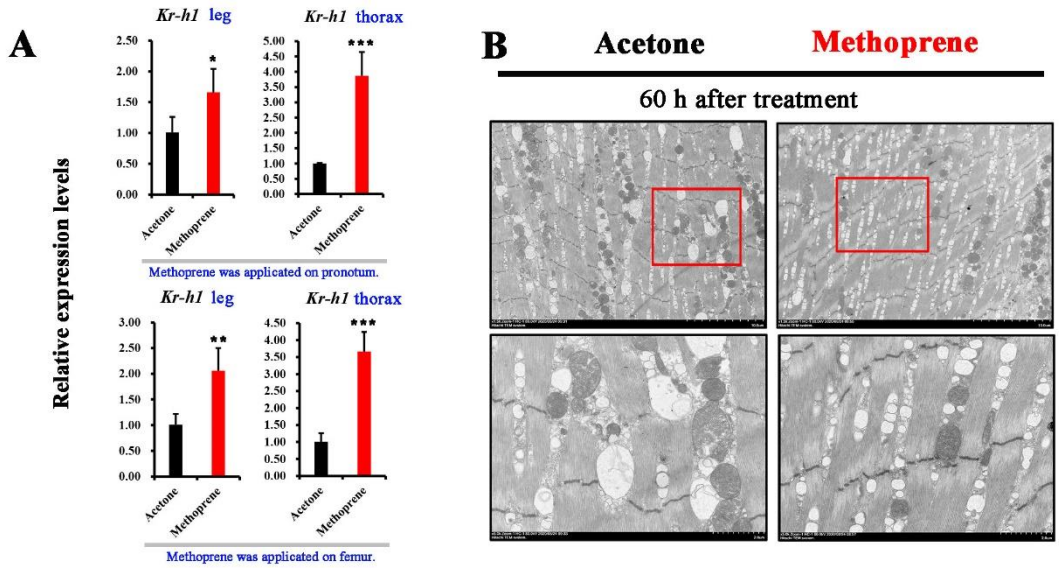

Fig. S5. JH application would not induce mitochondrial disruption and leg muscle fiber breakdown during starvation in winged female *A. pisum*. (A) Relative expression levels of *Kr-h1* in the legs and thoraxes of starved aphids at 12 h post methoprene treatment. Methoprene (100 ng/aphid) was applied at 24 h post eclosion, and the aphids were subjected to starvation. qPCR data are presented as the mean ± s.e.m. from 3 biological replicates (each replicate contains 10 aphids for the thoraxes or 50 aphids for the legs). Differences between 2 groups were determined by Student's t-test (*P < 0.05, ***P < 0.001). (B) Longitudinal ultrathin sections of leg muscles in the control and methoprene-treated aphids at 60 h after the treatment identified by TEM.

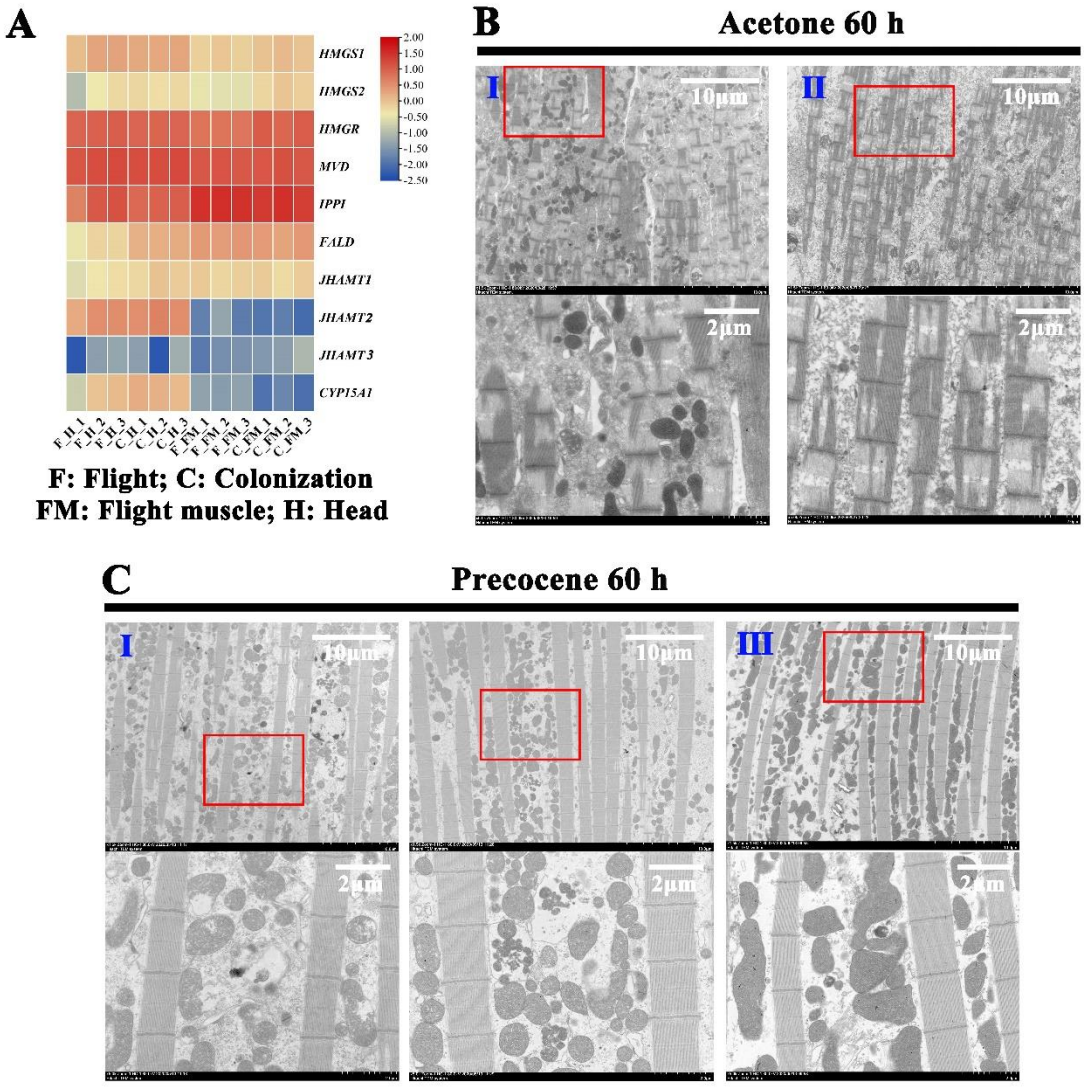

Fig. S6. JH biosynthesis level is relatively stable during colonization of winged aphids, which is necessary to colonization behavior. (A) Heat map representing the transcriptional changes (expression data from the RNA-seq of head and flight muscle) of genes involved in JH biosynthesis between "flight" and "colonization" aphids. (B and C) Effects of precocene II on histological changes of the flight muscles at 60 h after the treatment. Precocene (5 μg/aphid, dissolved in acetone) was topically applicated on the aphids 24 h post eclosion, and the treated aphids were placed in the feeding cages. I–III represents biological replications. Precocene inhibits colonization behavior of the winged aphids.

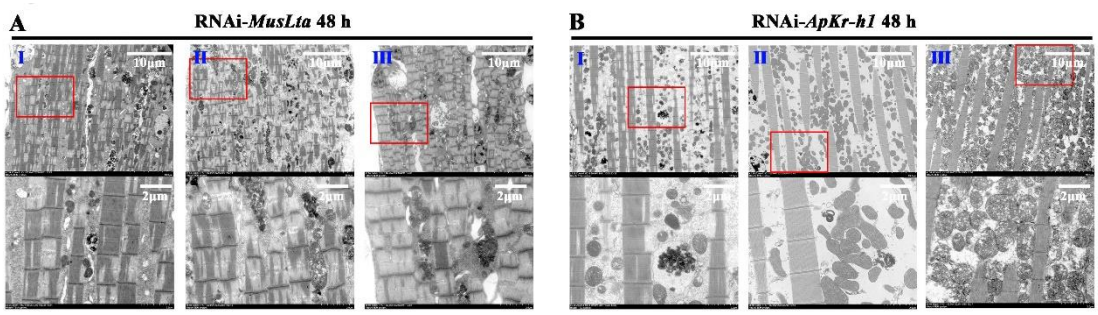

Fig. S7. RNAi-knockdown of *Kr-h1* delays flight muscle degeneration in winged *A. pisum*. TEM observation of the flight muscles of ds*Lta*- (A) and ds*Kr-h1*-injected (B) aphids at 48 h after dsRNA injection. Injection of dsRNA (6 μg/μL, 150 nL/aphid) was performed at 24 h after eclosion, and the treated aphids were placed in the feeding cages. I–III represents biological replications.

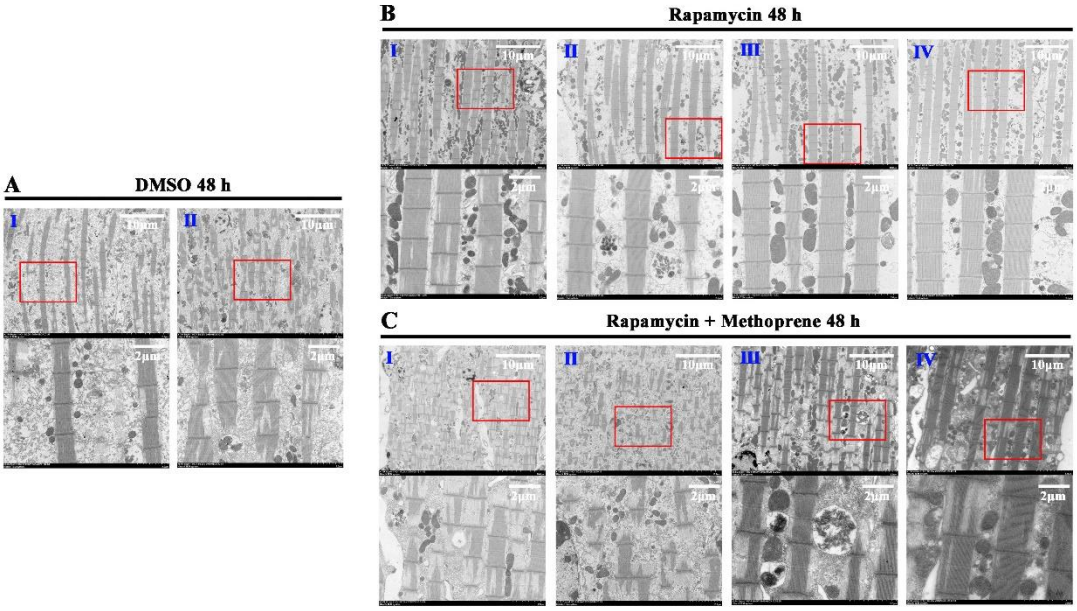

Fig. S8. Suppressing the TORC1 pathway by rapamycin inhibitor delays flight muscle degeneration in winged *A. pisum*. Histological changes of the flight muscles from DMSO-treated (A) aphids, rapamycin-treated (B) aphids, and methoprene-rescued aphids (C) at 48 h after the treatment. Rapamycin injection (2nM, 100 nL/aphid) and methoprene application (100 ng/aphid) were performed at 24 h after eclosion, and the treated aphids were placed in the feeding cages. I–IV represents biological replications.

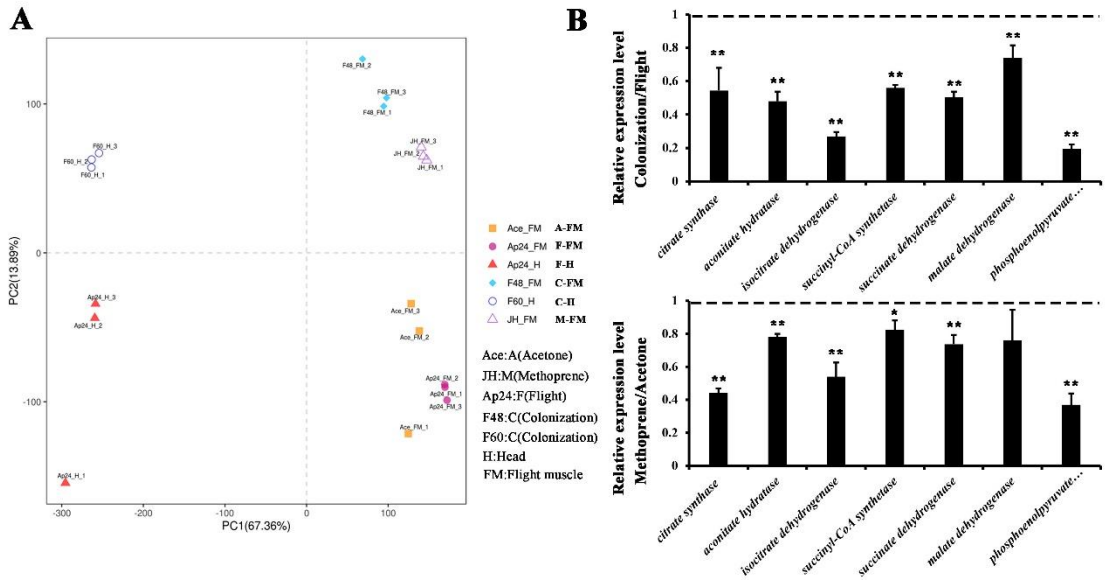

Fig. S9. Feeding and JH application down-regulates genes involved in the TCA cycle in the flight muscles of winged female *A. pisum*. (A) Principal component analysis (PCA) analysis of the whole RNA-seq samples involved in this study. (B and C) Transcriptome verification of selected genes involved in carbohydrate metabolism using qPCR. (B) Gene expression ratio between the aphids which are in the state of colonization and flight regarding the genes involved in the TCA cycle in the thoraxes. (C) Gene expression ratio of methoprene to acetone treated aphids regarding those same genes in the thoraxes at 24 h after the treatment. Differences between 2 groups were determined by Student's t-test (*P < 0.05, **P < 0.01). (CS, citrate synthase, geneID: 100162475; AH, aconitate hydratase, geneID: 100167414; ICDH, isocitrate dehydrogenase, geneID: 100161204; SCS, succinyl-CoA synthetase, geneID: 100168788; SDH, succinate dehydrogenase, geneID: 100165770; MDH, malate dehydrogenase, geneID: 100145825; PEPCK, phosphoenolpyruvate carboxykinase, geneID: 100160700)

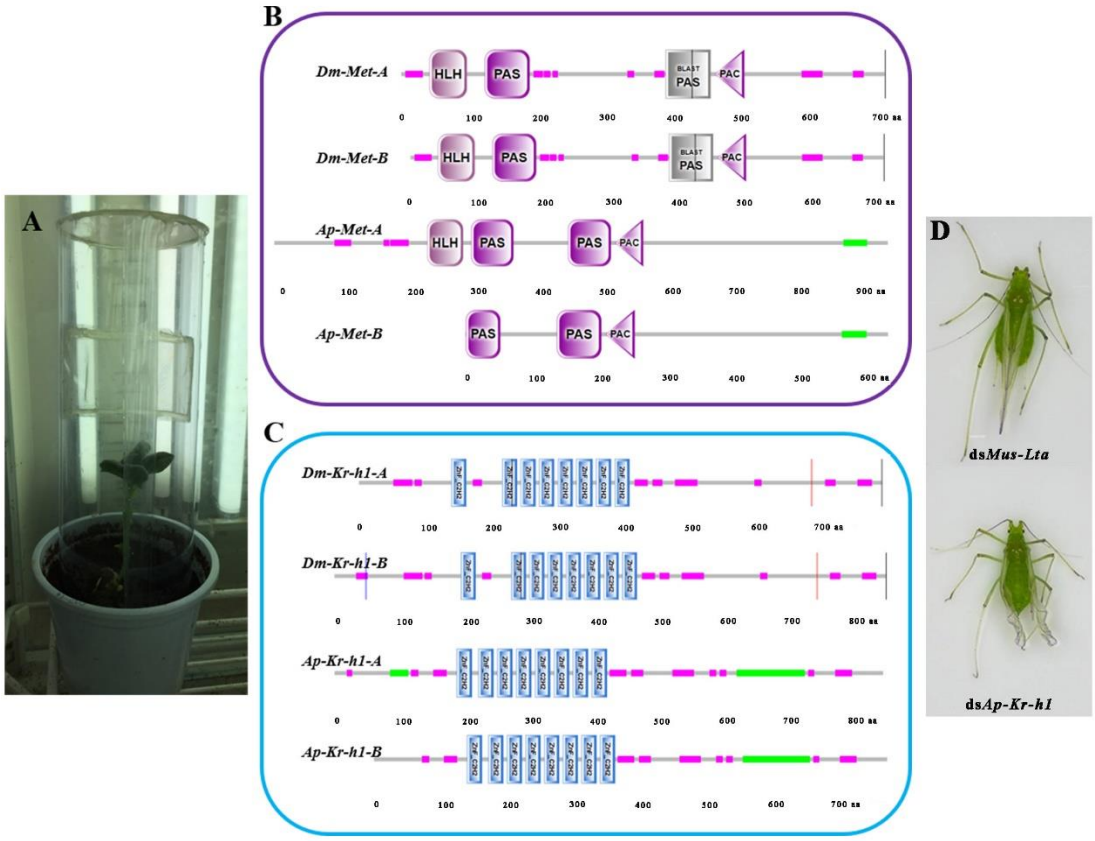

Fig. S10. The experimental devices and domain structure analysis of *ApMet* and *ApKr-h1* protein. (A) Cages supplied for the winged aphids to colonize and feed. Same as *Drosophila melanogaster*, *ApMet* and *ApKr-h1* have two transcriptional isoforms, respectively, named *ApMet* A/B and *ApKr-h1* A/B. Protein sequences are deduced by the ExPASy translation tool, and domains are predicted by the SMART tool. (B) Conserved domains of *DmMet* and *ApMet. Met* belongs to the basic helix–loop–helix (bHLH)-Per-Arnt-Sim (PAS) family of transcription factors. However, *ApMet* B lakes HLH domain. (C) Conserved domains of *DmKr-h1* and *ApKr-h1*. Both *DmKr-h1* A/B and *ApKr-h1* A/B contain eight C2H2-type zinc fingers (Znf) domains. (D) Phenotype of RNAi-*ApKr-h1*. Application of dsRNA was performed at 3rd nymph stage, and wing abnormal phenotype was obtained post eclosion.

Table S1. List of primers utilized in orthologue verification.

Fragment (bp)	Forward (5' to 3')	Reverse (5' to 3')
Ap-Met-A	AAGCTACCGGTGCAGTGTTG	CGTCAATCATATGCCTCAAGTGAAA
Ap-Met-B	AACCTATTCGCCTTTAATACGGAAA	CGTCAATCATATGCCTCAAGTGAAA
Ap-Kr-h1-A	CTTCAGTAGGCTGTTGACTGTTG	TTGTATAATGTGTACGTACGTTGCG
Ap-Kr-h1-B	TCGCACACTGTTCGTTATTTTTATT	TAATGTGTACGTACGTTGCGAAAAA

Table S2. List of primers utilized in qPCR.

gene	Forward (5' to 3')	Reverse (5' to 3')	Efficiency
q*Ap-JHAMT1*	CCATTAGTTGAGTTGTATAAATGT ATGGATAC	AATGTCTTTTATTTCATCTGGTGA ATACAC	*E* = 0.991
q*Ap-JHAMT2*	CAAGGCTGGATTTCGTATCA	TCATCTACAGCTCTGACGG	*E* = 0.985
q*Ap-JHAMT3*	TGCGGTTCTTCTTATTCGCTC	ATTAAGCAAGGCACCGACTTT	*E* = 0.844
q*Ap-Met*	TGCATCTGAACCTGGAATTG	ATCTTCAGTAACATCTTCCAATGT	*E* = 0.998
q*Ap-Kr-h1*	CGGTAGCGATAAGGAGAACA	GTCAGACAGCTGAAGCAATAC	*E* = 0.993
q*Ap-CS*	ACCACGAGGGTGGTAATGTA	CCATACCGGCACTGAATGAA	*E* = 0.990
q*Ap-AH*	CCAGACAAATTGAACGCCAG	AGCAATGACAACCGATCCAT	*E* = 0.995
q*Ap-ICDH*	AGGTCTAACACCCAGTGGAA	CGGCTATATCTGGAGCAGTTC	*E* = 0.989
q*Ap-SCS*	GTGGTGCTACTGCTTCTCAA	ATAGCACACACTTTGGGGTC	*E* = 0.991
q*Ap-SDH*	GGTGTGGGATGCTGGTAAAT	GCTACCGACAATCACACCAT	*E* = 0.997
q*Ap-MDH*	GTTCGGTCTAACAGATTCATTGC	CCGCCGATAACAGGAACATT	*E* = 0.992
q*Ap-PEPCK*	ACATGCTGATCTTAGGCGTG	CATCATCGCCATGTTGGTCT	*E* = 0.994
Ap-EF1α	TAGGAGGTATTGGAACAGTCC	TGTTTGCTGGTGCGAAAA	*E* = 1.030
q*Ap-rps20*	ATCAAAAGAGGCACAAAATCCGT	GCAATCATCTCGGAGCACAC	*E = 0.983*

Table S3. List of primers utilized in RNAi.

Fragment (bp)	Forward (5' to 3')	Reverse (5' to 3')
dsAp-Kr-h1 (307)	T7+AATGGTTCGGGAAGACGATG	T7+TTGGTGTCGACGAGTGATTG
dsMus-Lta (193)	T7+CACCCTCTCCACGAATTG	T7+TAGAAGATGCTGCTGTTTCA

T7 RNA polymerase promoter sequence: TAATACGACTCACTATAGGG.

Table S4. List of top pathways enriched in KEGG aggregation analysis from the comparative transcriptome of "colonization" vs "flight".

KEGG pathway	Background genes	**Up**-regulated genes	***P***-value
Proteasome	47	35	$2.59e^{-8}$
Protein processing in endoplasmic reticulum	126	35	$1.17e^{-5}$
Protein export	27	13	0.01099
Autophagy	27	12	0.02227
Phagosome	72	23	0.03952
KEGG pathway	Background genes	**Down**-regulated genes	***P***-value
Oxidative phosphorylation	125	53	$4.53e^{-6}$
2-Oxocarboxylic acid metabolism	22	14	0.00098
Citrate cycle (TCA cycle)	34	16	0.00461
Carbon metabolism	112	35	0.01178
FoxO signaling pathway	63	21	0.02693

Table S5. List of top pathways enriched in KEGG aggregation analysis from the comparative transcriptome of "methoprene" vs "acetone".

KEGG pathway	Background genes	**Up**-regulated genes	***P***-value
Proteasome	47	20	$1.05e^{-9}$
Protein processing in endoplasmic reticulum	126	20	0.00043
Endocytosis	130	20	0.00062
Autophagy	27	8	0.00089
ABC transporters	34	8	0.00310
KEGG pathway	Background genes	**Down**-regulated genes	***P***-value
Folate biosynthesis	32	6	0.00154
Carbon metabolism	32	6	0.00154
2-Oxocarboxylic acid metabolism	22	5	0.00184
Thiamine metabolism	14	4	0.00266
Cysteine and methionine metabolism	42	6	0.00520